COPPE
Instituto Alberto Luiz Coimbra de Pós-Graduação e Pesquisa de Engenharia
UFRJ

PRODUCTION OPTIMIZATION OF GAS-LIFTED OIL WELLS VIA EXTREMUM SEEKING CONTROL

Hans Christian Andersen da Silva

Dissertação de Mestrado apresentada ao Programa de Pós-graduação em Engenharia Elétrica, COPPE, da Universidade Federal do Rio de Janeiro, como parte dos requisitos necessários à obtenção do título de Mestre em Engenharia Elétrica.

Orientador: Alessandro Jacoud Peixoto

Rio de Janeiro
Março de 2019

PRODUCTION OPTIMIZATION OF GAS-LIFTED OIL WELLS VIA EXTREMUM SEEKING CONTROL

Hans Christian Andersen da Silva

DISSERTAÇÃO SUBMETIDA AO CORPO DOCENTE DO INSTITUTO ALBERTO LUIZ COIMBRA DE PÓS-GRADUAÇÃO E PESQUISA DE ENGENHARIA (COPPE) DA UNIVERSIDADE FEDERAL DO RIO DE JANEIRO COMO PARTE DOS REQUISITOS NECESSÁRIOS PARA A OBTENÇÃO DO GRAU DE MESTRE EM CIÊNCIAS EM ENGENHARIA ELÉTRICA.

Examinada por:

Prof. Alessandro Jacoud Peixoto, D.Sc.

Prof. Fernando Cesar Lizarralde, D.Sc.

Prof. Maurício Bezerra de Souza Jr., D.Sc.

RIO DE JANEIRO, RJ – BRASIL
MARÇO DE 2019

Silva, Hans Christian Andersen da

Production Optimization of Gas-Lifted Oil Wells Via Extremum Seeking Control/Hans Christian Andersen da Silva. – Rio de Janeiro: UFRJ/COPPE, 2019.

XIV, 57 p.: il.; 29, 7cm.

Orientador: Alessandro Jacoud Peixoto

Dissertação (mestrado) – UFRJ/COPPE/Programa de Engenharia Elétrica, 2019.

Bibliography: p. 50 – 57.

1. Oil Production Optimization. 2. Extremum Seeking Control. 3. Gas-Lifted Oil Wells. 4. Gas Lift. 5. Nonlinear Systems. I. Peixoto, Alessandro Jacoud. II. Universidade Federal do Rio de Janeiro, COPPE, Programa de Engenharia Elétrica. III. Título.

To my beloved mother Regina
and to the memory of my beloved
father Darcy, who taught me the
significance of education.

Acknowledgements

To my dearest wife Zulmira for the encouragement to pursuit my dreams and to be always by my side even during the darkest times. Many thanks!

I am grateful to my siblings and friends for helping me keep the focus and the belief that it was not too late.

To my colleagues, for all support and valuable discussions.

I would like to thank my employer BHGE for supporting my growth beyond ordinary business.

Finally, I must express my very profound gratitude to my thesis advisor D.Sc. Alessandro Jacoud Peixoto for having kept his office doors always open and provided me priceless guidance through the process of researching and writing this thesis. This accomplishment would not have been possible without him. Thank you.

Resumo da Dissertação apresentada à COPPE/UFRJ como parte dos requisitos necessários para a obtenção do grau de Mestre em Ciências (M.Sc.)

OTIMIZAÇÃO DA PRODUÇÃO DE PETRÓLEO EM POÇOS OPERADOS COM *GAS LIFT* VIA CONTROLE POR BUSCA EXTREMAL

Hans Christian Andersen da Silva

Março/2019

Orientador: Alessandro Jacoud Peixoto

Programa: Engenharia Elétrica

No presente trabalho, leva-se em consideração a elaboração de algoritmos de otimização em tempo real, em particular, aqueles baseados no Controle por Busca Extremal (ESC) para a otimização de poços de produção de petróleo operados com *gas lift*, devido à sua capacidade de superar as incertezas do sistema. Os esquemas de controle mantêm a produção de petróleo na vizinhança do ponto ótimo da Curva de Performance do Poço (WPC). A informação do gradiente da WPC não é utilizada *a priori*, sendo obtida através de perturbações periódicas inseridas na planta, assim como por estimativas de ajuste de curva. Este trabalho analisa o modelo não-linear de Eikrem para um poço de produção de petróleo operado por *gas lift*, fornecendo uma revisão bibliográfica abrangente e um modelo simplificado que representa o comportamento do modelo completo. Este novo modelo de segunda ordem que captura a dinâmica essencial do conhecido modelo de Eikrem é proposto para o qual um controle não-linear, baseado em linearização por realimentação, é empregado na malha interna para melhorar o transiente interno e permitir uma performance melhor do ESC na malha externa. Primeiramente supõe-se que os estados da planta estão disponíveis para realimentação, e então a estimação de estados baseada na leitura de sensores reais é considerada. Adicionalmente outros controles não-lineares são levados em conta e comparados com o controle através de linearização por realimentação com o intuito de proporcionar alternativas para a estratégia de controle da malha interna. Um novo algoritmo de controle por busca extremal sem perturbação é proposto para superar a limitação imposta pela baixa frequência da perturbação periódica presente no esquema clássico do ESC necessária para a separação da escala de tempo. A eficácia do esquema proposto é respaldada pelos resultados de simulações numéricas.

Abstract of Dissertation presented to COPPE/UFRJ as a partial fulfillment of the requirements for the degree of Master of Science (M.Sc.)

PRODUCTION OPTIMIZATION OF GAS-LIFTED OIL WELLS VIA EXTREMUM SEEKING CONTROL

Hans Christian Andersen da Silva

March/2019

Advisor: Alessandro Jacoud Peixoto

Department: Electrical Engineering

In this work, the design of on-line optimization algorithms are perceived, in particular, those based on Extremum Seek Control (ESC) for production optimization of gas-lifted oil wells due to its ability to overcome system's uncertainties. The control scheme maintains the oil production around the optimum point of the Well Performance Curve (WPC). The gradient information of the WPC is not used *a priori*, in fact it is obtained via periodic perturbation injected or on-line curve fitting estimation. This work investigates the nonlinear Eikrem's model for the gas-lifted oil well, providing a comprehensive literature study and a simplified model which captures the main behavior of the full model. This new second order model capturing the essential dynamics of the well known Eikrem's model is proposed for which a nonlinear controller based on feedback linearization is employed in an inner loop to improve the internal transient and allow a better ESC performance in the outer loop. At first, it is assumed that the plant state is available for feedback and then, a state estimation based on realistic sensor readings is considered. The gas-lifted oil well dynamic model was scrutinized in order to allow a deep understanding of the process providing a suitable choice for the measured variables to estimate the system states. Additionally, other nonlinear controllers are taken into account and compared to the feedback linearization control scheme in order to provide alternatives to the inner control loop strategy. A new dither-free ESC algorithm is proposed to overcome the low frequency limitation of the classic periodic perturbation ESC schemes required for time scale separation. The effectiveness of the proposed scheme is supported by simulation results.

Contents

List of Figures

List of Tables

List of Abbreviations

ESC	Extremum Seek Control, p. vii
ESP	Electric Submersible Pump, p. 2
GOR	Gas/Oil Ratio, p. 2
HGO	High Gain Observer, p. 6
HPF	High-Pass Filter, p. 42
IWIS	Intelligent Well Interface Standardisation, p. 30
LPF	Low-Pass Filter, p. 42
MPC	Model Predictive Control, p. 7
MPFM	Multiphase Flowmeter, p. 31
MPFM	Wet Gas Flowmeter, p. 31
NLO	Nonlinear Observer, p. 6
NMPC	Nonlinear Model Predictive Control, p. 7
PDG	Permanent Downhole Gauge, p. 30
PI	Productivity Index, p. 2
PI	Proportional Integral, p. 6
PLL	Phase-Locked Loop, p. 8
PTT	Pressure and Temperature Transmitter, p. 30
RP	Recommended Practice, p. 29
RTO	Real-Time Optimization, p. 43
SCM	Subsea Control Modules, p. 29

SIIS	Subsea Instrumentation Interface Standardisation, p. 29
SISO	Single-Input Single-Output, p. 16
TF	Transfer Function, p. 19
WCT	Wet Christmas Tree, p. 30
WPC	Well Performance Curve, p. vii

Chapter 1

Introduction

Petroleum, or just oil, is a complex mixture of hydrocarbons that can occur in liquid, gaseous or solid form. The most common form explored is the liquid form, called crude oil. The liquid and gaseous phases constitute the most important of the primary fossil fuels [6].

Oil started to be used primarily for illumination in mid-19^{th} century replacing the oils produced by animals (such as whales). The demand for a more convenient source of lubricants and illuminanting oil arise during the Industrial Revolution. At the begning of the 20^{th} century the advent of the internal-combustion engine led oil and gas industry to became the major supplier of energy. Oil was found to be a much more versatile form of fuel than anything previously available [6].

Nowadays, although oil represent major petrochemical feedstock, hydrocarbons are an essential resource worldwide as its derivatives are source of energy for industries and transportation on which the world economy depends [6, 7].

Most of the oil found in Brazil is located at subsea reservoirs. This led Petrobras to become a world leader company in petroleum exploration in deep and ultra-deep waters [8]. When reservoir pressure is not high enough to enable flow of oil to the surface or if the flow rate is not acceptable, the flow may be increased using artificial lift methods. Gas-lift is one of the main artificial lift technique for oil exploration that consists in inject gas through the annulus at the bottom of the production tubing decreasing the density of the fluid, thus making the mixture lighter decreasing the head loss facilitating greater production mass flow rates [7].

1.1 Artificial Lift via Gas Injection (*Gas Lift*)

Artificial lift is applied to oil production whenever the reservoir pressure is not enough to allow natural flow of oil towards surface or to increase production deemed not economic viable being applied for either greenfields and brownfields.

In the Oil & Gas industry there are mainly two kinds of artificial lift methods used: gas lift and pump assisted lift. One example of pump assisted system is the Electric Submersible Pump (ESP), which is being used more often due to its availability, growing flexibility and functionalities. Subsea engines are fed by a power source at surface via a specific power umbilical. The engine is connected to the subsea centrifugal pump which transfer energy to the fluid by pressurizing it, enabling easier flow to surface facility. This method is mainly used for production with high water levels, although there are ongoing studies to enable this technique to be used for fluids on high levels of Gas/Oil Ratio (GOR) [7]. ESP is a system composed of multistage centrifugal downhole pumps driven by a electrical motor and auxiliary equipment. Its operating principle is to use the centrifugal pump to generate the required bottom-hole pressure that allows a desired flow rate. The use of a variable-speed drive allows a more flexible production operation. It is one of the most versatile of the major oil production artificial lift methods [9].

Gas lift can be of two types: intermittent and continuous. In this master thesis, "gas lift" means the continuous gas lift. Gas lift is a widely used technique of artificial lift due to its relatively low cost. It is suitable for production wells with high levels of sand and GOR, up to 2.600m of water depth producing from 1 to $1.700m^3$/day [7]. Figure 1.1 shows a typical gas-lift system.

Gas-lift is based on injecting high pressurized gas into the lower part of the production tubing through a gas lift valve or orifice to gasify oil from the injection point to the surface. Increasing the amount of gas in the production tubing, i.e. increasing GOR, reduces the average gradient of hydrostatic pressure. By reducing the back pressure in the wellbore caused by flowing fluids into the production tubing, the inflow from reservoir is increased consequently increasing oil production [7, 10–12].

Gas lift is best applied when one or more of these characteristics are present:

- Reservoir fluid has a high gas content;
- Well has a good reservoir Productivity Index (PI) ;
- Reservoir pressure can be maintained;
- Fluid has entrained solids detrimental to pumps (fines, scale, paraffin);
- Wellbore work-over cost is high.

Some advantages of gas lift described in [13]:

- Gas-lift requires few moving parts, and therefore is suitable also when solids (such as sand) are produced;

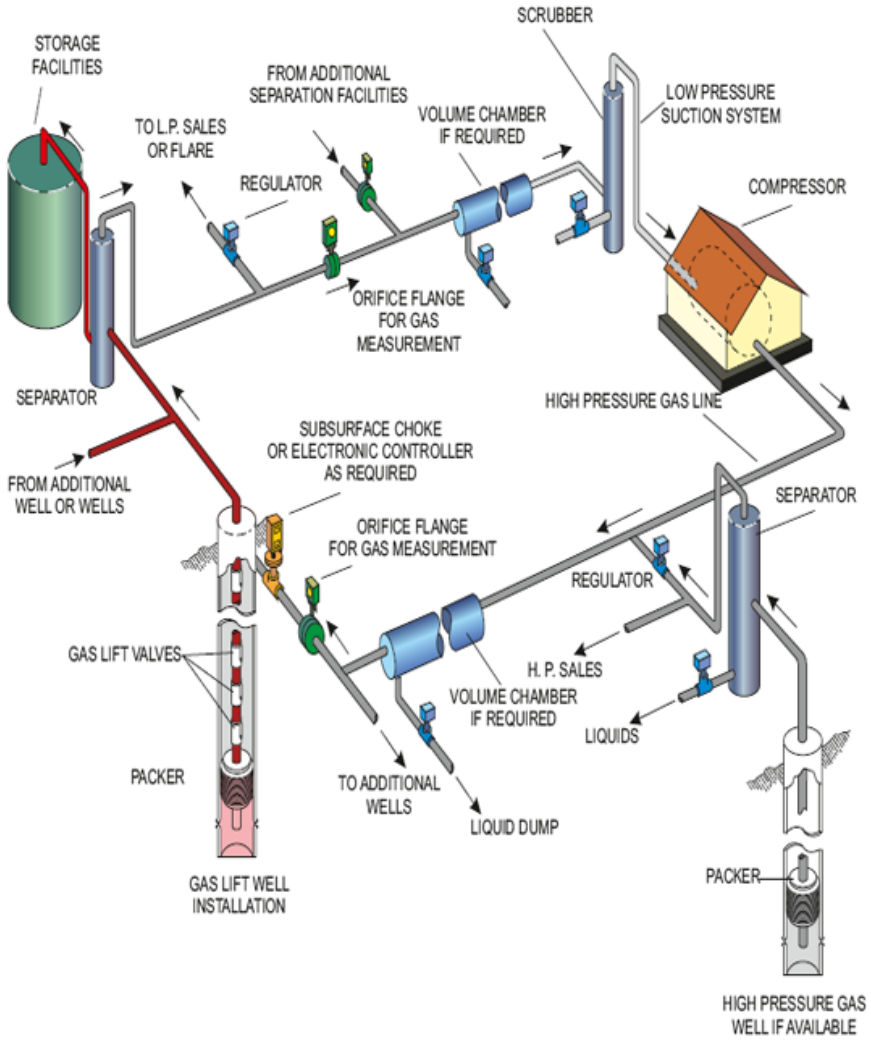

Figure 1.1: Gas-lift system illustration [1].

- Gas-lift works well in a well with a multi-inclination trajectory, where installing a bottomhole pump may be difficult;
- Gas-lift wells have downhole equipment with low cost and long service life. The major equipment is the gas compressor, which is located on the surface (offshore: on the production unit), which allows for easy maintenance, while the downhole equipment mainly consists of valves;
- Gas-lift is very flexible to changes in well conditions and production rates.

There are some known issues with gas lift systems. The larger the number of wells the higher the capacity of gas compressor is required since the gas is circulated through all wells. Gas lift can result in highly oscillating well flow when the pressure drop in the tubing is gravity dominated and there is a large annulus volume filled with compressible gas. This type of oscillations is described as casing-heading instability [2], described below:

(1) Gas from the annulus starts to flow into the tubing. As gas enters the tubing the pressure in the tubing falls, accelerating the inflow of gas-lift.

(2) If there is uncontrolled gas passage between the annulus and tubing, the gas pushes the major part of the liquid out of the tubing, while the pressure in the annulus falls dramatically.

(3) The annulus is practically empty, leading to a negative pressure difference over the injection orifice blocking the gas flow into the tubing. Due to the blockage, the tubing becomes filled with liquid and the annulus with gas.

(4) Eventually, the pressure in the annulus becomes high enough for gas to penetrate into the tubing, and a new cycle begins.

This oscillation can damage downstream processing equipment and causes severe loss of production compared to steady production. Figure 1.2 shows an illustration of a well operated with gas-lift.

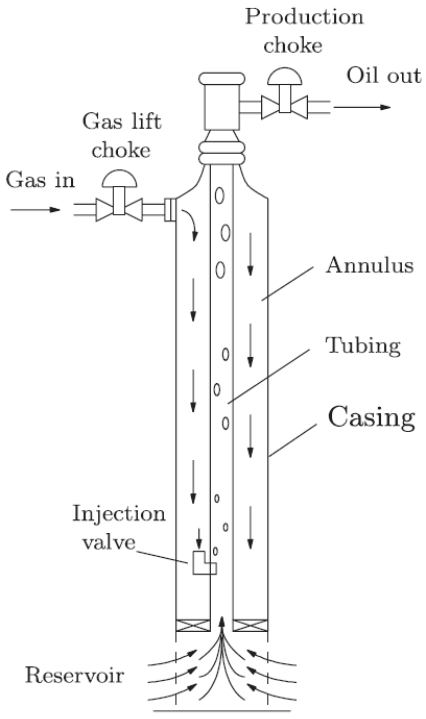

Figure 1.2: Gas lift well [2].

Gas lift is widely used in Brazil, having more than 80% of the Campos Basin wells applying this method of artificial lift [14]. Although this technique can be considered mature, little information can be found in literature regarding automatic control of an actual offshore process which can lead to infer the control system is still mainly manual relying on operators solely skills and some offline calculations. The

implementation of an automatic control would allow unprecedented steady peak of production with much less effort.

1.2 Oil Production Optimization

1.2.1 Well Performance Curve

Gas lifted wells optimization can only be pursued once the concept of Well Performance Curve is established. The WPC relates gas injection flow rates with oil flow at the well head, i.e. the produced oil. This makes the WPC the main mean in finding operating points for a gas-lifted well [9].

Figure 1.3 illustrate a typical well production curve. The varying outflow is due to a combination of the hydrostatic pressure head and the friction pressure drop. It can be observed that once the injection of gas is started it results in a fluid density reduction with modest friction pressures and oil production is increased, continued increase in the lift gas supply makes friction pressure losses in the tubing dominant and the production rate starts declining. This effect makes WPC to have a peak, which would be the theoretical maximum production or the optimum injection rate, if production constraints are not considered [9]. In practice, however, an economical region of operation is delimited by factors such as: supply cost of lift gas, limited actuation of gas compressors, high-pressure gas damage risks in the well, and water treatment costs [9, 15].

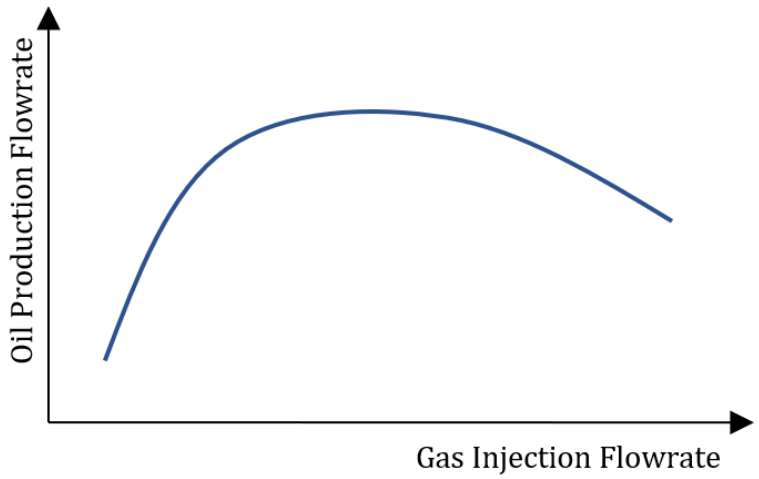

Figure 1.3: Typical Well Performance Curve.

Although undeniable importance of WPC for oil production optimization, many phenomenological model parameters are unknown and there is also limited understanding of some of the physics involved. Hence, pure physical WPC models

are uncommon and well performance curves are usually generated numerically by simulation software [9].

1.2.2 Gas-Lifted Oil Well Model and Optimization

The automatic control to stabilize gas-lifted oil wells introduced in [16], considered a model based controller to command the production and injection choke valves, resulting in an increased production due to a more efficient usage of gas lift. In [17], the stabilization of gas lifted wells was evaluated for multiple wells using different approaches: one for downhole pressure control and other for control of the gas pressure in the annulus. A dynamic model of a gas lift well for casing head instabilities based on the balance of masses of oil and gas in the tubing and in the annular was presented in [18]. In this work a Nonlinear Observer NLO was combined with a conventional Proportional Integral (PI) control of downhole pressure to stabilize the multiphase flow and increase production. This model was revised by [2] by the insertion of the flow of the oil from the reservoir to the tubing. In [19] a different model for gas-lifted oil wells was developed based on Navier-Stokes equations.

Scibilia et al. [20] proposed a stabilization method using topside measurements based on Eikrem previous findings, but introducing a High Gain Observer (HGO) to drop assumptions of [18] related to measurements of states. A controllability analysis was performed in [21] concluding that a secondary manipulated variable does not improve stabilization of the gas-lifted oil wells significantly. The bottom-hole pressure provided the best results in terms of controllability when using topside measurements for casing-heading instability prevention. Some modifications to the model were proposed in [22] to take head loss into account. This modified models was used for the study of a multivariable predictive control with quality constrains. Other additional modifications were made by [13], including water in the model including a third phase to the system that used to considers only a two-phase scenario with production of oil and gas. It also aimed to compare dynamic to static optimization, but results from the three proposed dynamic optimization methods were not conclusive, showing only little indications of performance improvement.

In [23] the efforts were to better evaluate the impact of control of gas-lift choke and also has included more system constraints and a statistical estimator for the downhole pressure. An algorithm for flow stabilization was presented in [24] whithout setting a value for the bottom pressure. A novel model was proposed in [25] for predicting the temperature profile in gas lift wells by a combination model of heat balance and linear temperature profile estimation. In [26] a novel mathematical model was proposed for describing the behaviors of the gas-lift system by discretizing

the differential equations describing the gas lift dynamics simultaneously with respect to both time and space, dropping the need of the homogeneous assumption across the whole tubing.

Just like several models have been developed to characterize a gas-lifted oil well, different approaches arose related to production control and optimization. Model Predictive Control (MPC) is often used by the industry as an effective mean to deal with multivariable constrained control problems [27] and an expected consequence is to have a development of a Nonlinear MPC (NMPC) applied to gas-lift oil production like proposed in [28], [22] and [29]. Mixed-Integer Linear or Nonlinear programing and hydbrid systems were the focus of [30], [31], [32], [33], [34], [13], [35], [11], and [9]. There is also some study related to genetic algorithms in [30] and in [36]. It also remarkable that a considerable part of the available literature also encompass optimization of allocation of gas-lift among multiple wells like in [31], [34] and in [37] which proposed a control strategy for the pressure of the gas lift manifold and a software sensor to indirectly measure the gas-mass flow-rate available for artificial lifting besides a module for identification of well performance curves from downhole pressure measurements. A survey of methods and techniques developed for the solution of the continuous gas-lift optimization problem was presented in [38]. Gas lift optimization has been scrutinized in many several ways, including real time optimization of gas-lift [39], gas-lift network optimization [40, 41] and gas-lift optimization by marginal GOR control [42]. There are also research related to optimization for other types of oil related systems (e.g. oil reservoir waterflooding, oil field development, separation systems) [43–46].

In this context it is possible to find simulators that mimic the systems under study. Among them [47] proposed a simulator of intermittent gas-lift and [48] presents a platform for gas-lifted oil optimization in real time.

Despite the great amount of research on this area, it is a very relevant fact that WPC cannot be obtained beforehand, but only after a well is individually tested. The difficulty of estimating the WPC has fostered the search for a robust real-time method that enable the oil production flow values around the optimum of the WPC [5, 49]. Being ESC model free, it has proven to be both robust and effective in many different application domains. One of the first and most popular applications is the optimization of internal combustion engines, however ESC is suitable for a number of application such as autonomous vehicles, mobile robots, jet instability control, neural network/fuzzy logic, etc. [50].

Several articles scrutinized applicability, stability, performance and limitations in ESC like [51], [52] and [53]. Important contributions in extremum seeking control can be found in [54–57] with particular emphasis for [56] when the method was generalized for a class of dynamic plants stabilizable via state feedback. The

intention was to generate a closed-loop system with sufficiently fast dynamics in order to behave approximately as a static plant. In [58] it was shown that global asymptotic stability of the closed-loop system of plant and perturbation extremum seeking controller with respect to the optimal steady-state plant performance can be obtained for any plant that satisfies the assumptions in that work. In [59] an ESC method was presented for steady-state performance optimization of general nonlinear plants with periodic steady-state outputs. A local extremum-seeking control method was proposed in [60] for steady-state performance optimization of general nonlinear plants with time-varying steady-state outputs. An ESC scheme was proposed for optimization of gas-lifted wells in [5] has being followed by [15] and [61], proposing a PLL (Phase-Locked Loop) in order to achieve a faster convergence of the ESC around the optimal production point. A method was proposed by [62] to make ESC robust to disturbances, by removing the effect of the disturbance with a priori information of the disturbance model. This made the proposed model to be restrictive as it requires the disturbance model to be known. A distributed extremum seeking algorithm was presented by [63] for the problem of production optimization of multiple gas lifted wells. A ditter-free ESC approach using least squares fits for gardient estimation was presented in [4]. In [64] a feedback real time Optimization using a novel steady-state gradient estimate was proposed. Those new approaches represent new alternatives for the gas-lifted oil wells production optimization based on ESC scheme.

1.3 Dissertation Purpose

The main idea of present work is to use as an inner loop a controller based on feedback linearization in order to obtain faster transient response so that the outer loop, a real-time non model based algorithm relying on Extremum Seeking Control, is developed to control the gas lift flow injection. In that way, the ESC outer loop provides the set-point to the inner loop, maximizing the oil production.

In this research we get a deep understand of plant dynamics to find multiple ways to improve ESC performance applied to a gas-lifted oil plant for oil production optimization. The system considered is based on the mathematical model of a gas lift well described by Eikrem et al. [2] and modified by Ribeiro [22]. The controller proposed focus on taking advantage of actual sensor readings data and some estimated states to stabilize and accelerate the plant dynamics in order to reach the optimal point and, consequently, maximize the production. Scenarios are tested by simulation as an evaluation of their performance.

1.4 Notation and Terminology

The following notation and basic concepts are employed: **(1)** The symbol "s" represents either the Laplace variable or the differential operator "d/dt", according to the context. **(2)** The output y of a linear time invariant (LTI) system with transfer function $H(s)$ and input u is given by $y = H(s)u$. **(3)** $\pi(t)$ is any exponentially decreasing signal, i.e., a signal satisfying $|\pi(t)| \leq \Pi(t)$, where $\Pi(t) := Re^{-\lambda t}$, $\forall t$, for some scalars $R, \lambda > 0$. **(4)** Classes of $\mathcal{K}, \mathcal{K}_\infty, \mathcal{L}$ functions are defined in accordance with [65], in particular, a function $\beta : \mathbb{R}^+ \to \mathbb{R}^+$ belongs to class $\mathcal{L}$ if it is continuous, strictly decreasing and $\lim_{t\to\infty} \beta(t) = 0$. Furthermore, a function $\alpha : \mathbb{R}^+ \to \mathbb{R}^+$ belongs to class $\mathcal{K}$ if it is continuous, strictly increasing and $\alpha(0) = 0$.

1.5 Document Outline

The present document is organized as follows. First, in order to provide to the reader the necessary contents for understanding the application of the results obtained by this study, an overview of control and optimization of oil production in gas lift well was provided in Chapter 1. The mathematical model developed by [2] for a gas-lift well is presented in Chapter 2. Static models and a simplified reduced order model that mimics the dynamics of the standard models are also evaluated. In Chapter 3 the controller required for accelerate the inner dynamics before applying the ESC approach is presented and the ESC theory is described encompassing classic and alternative methods applied to gas lift model. Chapter 3 is also dedicated to a variation of the Extremum Seeking Control algorithm and its application on the oil production. In sequel, the ESC is introduced and applied to the dynamic model and the control strategy developed is evaluated via numerical simulations. Finally, Chapter 4 presents some concluding remarks and thoughts on future work.

Chapter 2

Dynamic Model of a Gas-Lifted Well

2.1 Eikrem's Model for Well Production

This chapter aims to present all main elements and components of a gas-lifted well. Eikrem et al. [2] have developed a non-linear model for a gas-lifted well while studying casing head phenomenon described in 1.1. The dynamics of this model has been validated being widely used in literature. It should be noted, however, that referenced model is just complex enough to fit the original purpose. Main simplifications applied to the model and also present in this work are considered are listed below.

Reservoir Pressure p_r is deemed constant

- Reservoir dimensions are very large and therefore its pressure decreases very slowly during the years

Upstream choke pressure p_s is deemed constant

- Assuming there is a feedback controller keeping it steady or due to the own line characteristics.

Flows trough the valves are deemed unidirectional

- Valves are assumed to behave as check valves allowing the flow in only one direction.

Production discharge is deemed biphasic

- Although production is characterized by a three-phase flow (oil, water and gas), the model considers water and oil as a single phase.

Gas/Oil Ratio (GOR) r_{go} is deemed constant

Gas and Oil masses vary slowly

Molar weight of Gas M is deemed constant

Oil density ρ_o is deemed constant

- The oil is considered incompressible.

Temperature of Anular and Production Tubing is deemed constant

The gas lift process described in Section 1.1 is modeled mathematically by three states: x_1 is the mass of gas in the annulus; x_2 is the mass of gas in the tubing, and; x_3 is the mass of oil in the tubing above injection port. The model can be understood as having four parts: mass balance model of the phases, densities models, pressures models and flows models. The state equations of the system are listed below:

$$\dot{x_1} = w_{gc} - w_{iv}, \tag{2.1}$$

$$\dot{x_2} = w_{iv} + w_{rg} - w_{pg}, \tag{2.2}$$

$$\dot{x_3} = w_{ro} - w_{po}, \tag{2.3}$$

where $u = w_{gc}$ is a constant mass flow rate of lift gas into the annulus (control input), w_{iv} is the mass flow rate of lift gas from the annulus into the tubing, w_{rg} is the mass flow rate of gas from the reservoir into the tubing, w_{pg} is the mass flow rate of gas through production choke, w_{ro} is the mass flow rate from the reservoir into the tubing and w_{po} is the mass flow rate of produced oil through the production choke. Physical variables of the model presented are show in Figure 2.1. The plant output is the production choke w_{po} as per the equation below:

$$y = w_{po}. \tag{2.4}$$

The system flows are modeled by:

$$w_{gc} = u \text{ (flow rate of gas lift)}, \tag{2.5}$$

$$w_{iv} = C_{iv}\sqrt{\rho_{ai}\ max\{0,\ p_{ai} - p_{wi}\}}, \tag{2.6}$$

$$w_{pc} = C_{pc}\sqrt{\rho_m\ max\{0,\ p_{wh} - p_s\}}\ u_c, \tag{2.7}$$

$$w_{pg} = \frac{x_2}{x_2 + x_3} w_{pc}, \tag{2.8}$$

$$w_{po} = \frac{x_3}{x_2 + x_3} w_{pc}, \tag{2.9}$$

$$w_{ro} = C_r\sqrt{\rho_o(p_r - p_{wb})}, \tag{2.10}$$

$$w_{rg} = r_{go} w_{ro}, \tag{2.11}$$

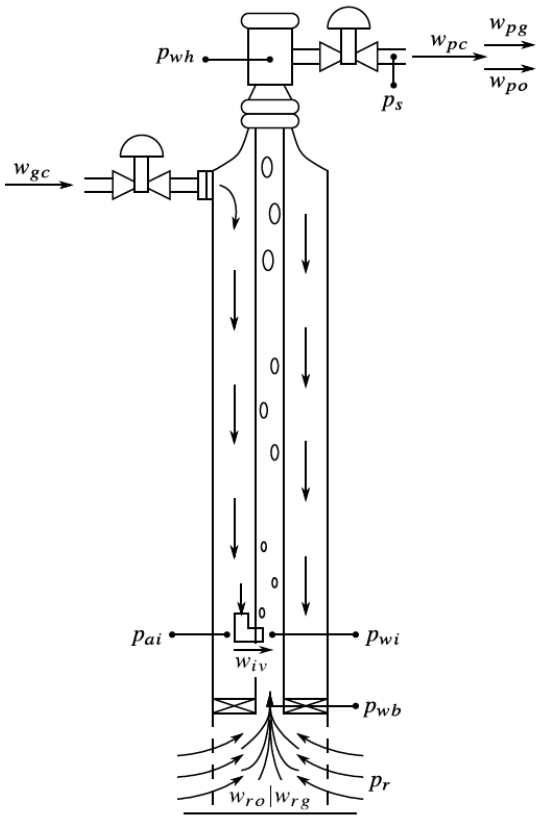

Figure 2.1: Physical variables of the model [3] (adapted from [2]).

where C_{iv}, C_{pc} and C_r are positive constants, being the flow capacity of injection, production valves and reservoir respectively, u_c is the production choke opening ($u_c(t) \in [0, 1]$), ρ_{ai} is the density of gas in the annulus at the injection point, ρ_m is the density of oil/gas mixture at the top of the tubing (wellhead), ρ_o is the density of the oil in the reservoir, p_{ai} is the pressure in the annulus at the injection point, p_{wi} is the pressure in the tubing at the gas injection point, p_{wh} is the pressure at the wellhead, p_s is the pressure downstream production choke - it is possibly the pressure at manifold bore which is assumed that either there is a control to maintain its value constant or that the system architecture is such that this pressure varies very slowly, p_r is the pressure in the reservoir - also assumed to be slowly varying and therefore treated as constant, p_{wb} is the pressure at the bottom of the tubing (downhole), r_{go} is the gas oil ratio of the flow from the reservoir.

The densities of the system are modeled as follows:

$$\rho_{ai} = \frac{M}{RT_a} p_{ai}, \tag{2.12}$$

$$\rho_m = \frac{x_2 + x_3 - \rho_o L_r A_r}{L_w A_w}, \tag{2.13}$$

$$\rho_o = \frac{1}{v_o}, \tag{2.14}$$

where M is the molar weight of the gas, R is the gas constant, T_a is the temperature in the annulus, L_r is the length from the reservoir to the gas injection point, A_r is the cross-sectional area of the tubing below the injection point, L_w is the length of the tubing above the injection point, A_w is the cross-sectional area of the tubing above the gas injection point and v_o is the specific volume of the oil.

The pressures of the system are modeled as follows:

$$p_{ai} = \left(\frac{RT_a}{V_a M} + \frac{gL_a}{V_a}\right) x_1, \tag{2.15}$$

$$p_{wh} = \frac{RT_w}{M} \frac{x_2}{L_w A_w + L_r A_r - v_o x_3}, \tag{2.16}$$

$$p_{wi} = p_{wh} + \frac{g}{A_w}(x_2 + x_3 - \rho_o L_r A_r), \tag{2.17}$$

$$p_{wb} = p_{wi} + \rho_o g L_r, \tag{2.18}$$

where g is the acceleration of gravity, L_a is the length of the annulus, V_a is the annulus volume and T_w is the temperature in the tubing.

Considering the model presented in this section (2.1) – (2.3), it can be verified that all masses flow rates result from the differential pressure between some points of the tubing. Therefore for the oil to be able to flow from the reservoir into the tubing and downstream the following is required:

$$p_r > p_{wb} > p_{wi} > p_{wh} > p_s, \tag{2.19}$$

$$p_{ai} > p_{wi}. \tag{2.20}$$

The maximum functions of the model represent the unidirectional flow assumption. The gas injection w_{gc} can be controlled by the injection choke actuation directly. However the production choke is considered to be permanently open to maximize the production, i.e. $u_c(t) = 1$. Therefore equations 2.6 and 2.7 can be rewritten as:

$$w_{iv} = C_{iv}\sqrt{\rho_{ai}(p_{ai} - p_{wi})}, \tag{2.21}$$

$$w_{pc} = C_{pc}\sqrt{\rho_m(p_{wh} - p_s)}. \tag{2.22}$$

2.1.1 Well Parameters

Oil well parameters used in this work are as shown in Table 2.1. Table 2.2 provides parameter's descriptions.

Table 2.1: Oil well parameters used [5].

Parameter	Value	Unit
A_r	0.203	m^2
A_w	0.203	m^2
C_{iv}	15×10^-5	–
C_{pc}	1.655×10^-3	–
C_r	2.623×10^-4	–
g	9.81	m/s^2
L_a	230.87	m
L_r	132	m
L_w	1217	m
M	0.028	kg/mol
μ	1×10^-3	cP
p_r	2.5497295×10^7	Pa
p_s	3.704669×10^6	Pa
R	8.314	$J/Kmol$
r_{go}	0.0818	–
ρ_o	923.9	kg/m^3
T_a	293	K
T_w	293	K
V_a	29.012	m^3
$x_1(0)$	3735.2	kg
$x_2(0)$	8729.5	kg
$x_3(0)$	109300	kg

2.1.2 Model Modifications

Eikrem et al. [2] model has been developed for casing head instabilities evaluation, once this goal has been achieved several simplifications took place. One of the most remarkable simplification is that friction is not considered at all. Looking at Figure 1.3 it can be concluded that friction is more significant at high flow rates. Therefore pressure drop due to friction must be considered to obtain a more precise model of the fluid flow and pressures in the tubing.

Ribeiro [22] proposed some model modifications to take friction into account as follows:

$$p_{wi} = p_{wh} + \frac{g}{A_w}(x_2 + x_3 - \rho_o L_r A_r) + h_f L_w, \tag{2.23}$$

$$p_{wb} = p_{wi} + \rho_o g L_r + h_f L_r, \tag{2.24}$$

where h_f is Darcy-Weisbach equation - an empirical equation, which relates the head loss, or pressure loss, due to friction along a given length of pipe to the average velocity of the fluid flow for an incompressible fluid. In a cylindrical pipe of uniform

Table 2.2: Well parameters descriptions.

Parameter	Description
A_r	Tubing cross-section area below injection point
A_w	Tubing cross-section area above injection point
C_{iv}	Injection valve flow capacity
C_{pc}	Production choke injection valve flow capacity
C_r	Flow capacity of interface reservoir/tubing
g	Acceleration if gravity
L_a	Annulus length
L_r	Length from reservoir to gas injection point
L_w	Tubing length above injection point
M	Gas lift molar weight
μ	Mixture viscosity
p_r	Reservoir pressure
p_s	Pressure downstream production choke
R	Gas constant
r_{go}	Gas oil ratio
ρ_o	Density of the oil in the reservoir
T_a	Annular temperature
T_w	Tubing temperature
V_a	Annular volume

diameter $D = 2\sqrt{A_r/\pi}$, flowing full, the pressure loss due to viscous effects Δp is proportional to length L and can be characterized by the Darcy–Weisbach equation:

$$h_f = f_D \frac{\rho_m}{2} \frac{v^2}{D}, \tag{2.25}$$

f_D is the friction factor, ρ_m is the density of the fluid, v is the mean flow velocity of the fluid and D is the internal diameter of the pipe. The friction factor is dependent on the flow regime, Reynolds number (Re) and pipe absolute roughness. Reynold number is defined as below:

$$Re = \frac{\rho_m v D}{\mu}, \tag{2.26}$$

where μ is the viscosity of the fluid.

For a laminar flow ($Re < 2300$), f_D is independent of pipe roughness, being given by:

$$f_D = 64/Re, \tag{2.27}$$

For turbulent flow in smooth pipes (roughness $\epsilon = 0$), the Blasius correlation can be used to determine the friction factor:

$$f_D = \frac{0.316}{Re^{0.25}}, \tag{2.28}$$

which is valid for $Re \leq 10^5$ [66], representing a small difference from Ribeiro's proposed modification, justified by the fact that in the present work Re never reaches this limit, hence this is the only equation needed for turbulent flow.

2.1.3 The Class of Nonlinear System

From a Control Theory perspective, the model of the gas lift oil well may be described as a Single-Input Single-Output (SISO) system.

$$u = w_{gc},$$
$$y = w_{po},$$

corresponding to the gas inflow through the gas injection choke and the oil outflow at the production choke, respectively.

From (2.8) and (2.9), $w_{pg} = \frac{x_2}{x_3} w_{po}$. Therefore, the system (2.1) – (2.4) can be rewritten as follows:

$$\begin{aligned}
\dot{x}_1 &= u - \varphi_1(x_1, x_2, x_3), \\
\dot{x}_2 &= \varphi_1(x_1, x_2, x_3) + r_{go}\varphi_2(x_2, x_3) - \frac{x_2}{x_3}\varphi_3(x_2, x_3), \\
\dot{x}_3 &= \varphi_2(x_2, x_3) - \varphi_3(x_2, x_3), \\
y &= \varphi_3(x_2, x_3),
\end{aligned} \tag{2.29}$$

where $\varphi_1 = w_{iv}$ is obtained from 2.21, 2.12, 2.15, 2.17 and 2.16; $\varphi_2 = w_{ro}$ is obtained from 2.10, 2.18, 2.17, 2.16; $\varphi_3 = w_{po}$ is obtained from 2.9, 2.22, 2.13, 2.16.

2.2 Open Loop Numerical Evaluation

2.2.1 Nonlinearities Evaluation

Varying x_2 and x_3 within the region of interest allow further knowledge of the model variables. In Figure 2.2a, it is evident that term $p_{wh} - p_s$ increases with x_2 and x_3 and a nonlinear relationship is observed for high values of x_2 and x_3.

On the other hand, the density of the mixture (oil and gas) ρ_m reveals a linear function according to Figure 2.2b. Moreover, for a fixed x_2, ρ_m is almost constant while for a given x_3, ρ_m increases with x_2, see Figure 2.2b.

For the oil flow rate w_{po}, a nonlinear relationship is evident in Figure 2.2c, $\forall x_2, x_3$ in the region of interest and, in particular for values around the coordinates $(1, 5.5) \times 10^4$, where the effect of the maximum function appearing in the definition of w_{po} generates the zero values.

Likely the density of the mixture ρ_m, the oil flow rate from the reservoir to the tubing w_{ro} can also be approximated by a linear function of x_2 and x_3. In fact, it can be observed in Figure 2.2d that w_{ro} is inversely proportional to x_2 and x_3, which makes sense considering as much tubing is filled with gas and oil, there will be less space for flow from the reservoir. The curve of Figure 2.2d is slightly nonlinear and shows that w_{ro} tends to zero when x_2 and x_3 are increased.

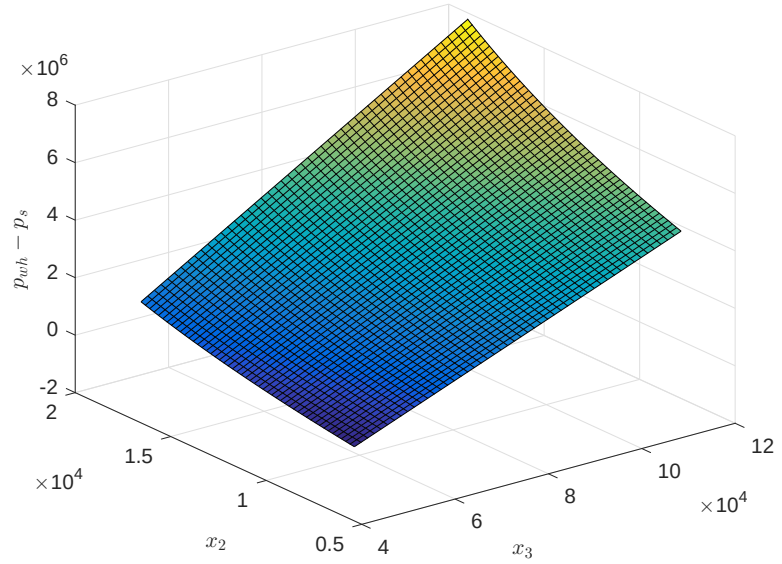

(a) $p_{wh} - p_s$ evaluation.

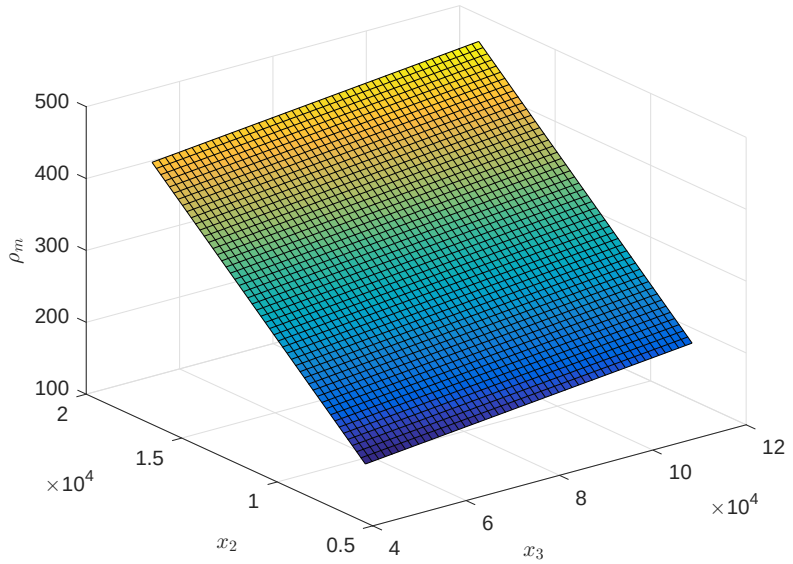

(b) ρ_m evaluation.

Figure 2.2: Model nonlinear terms evaluation against x_2 and x_3.

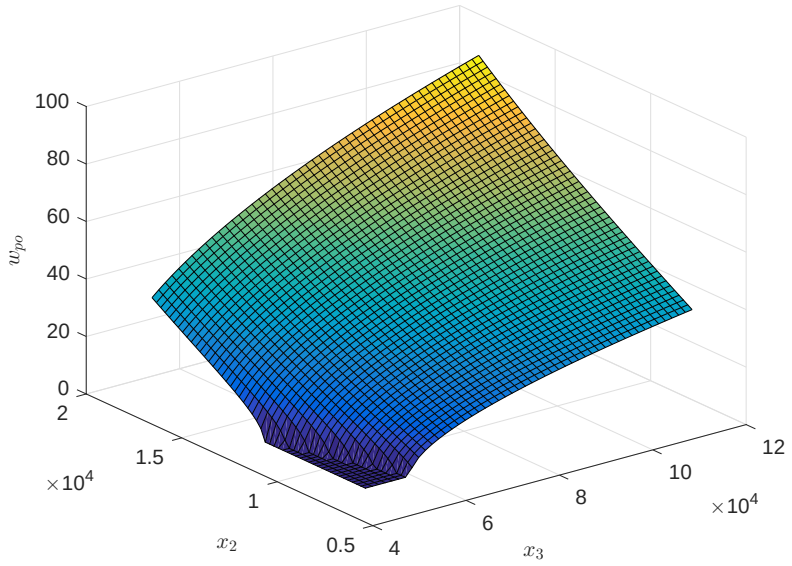

(c) w_{po} evaluation.

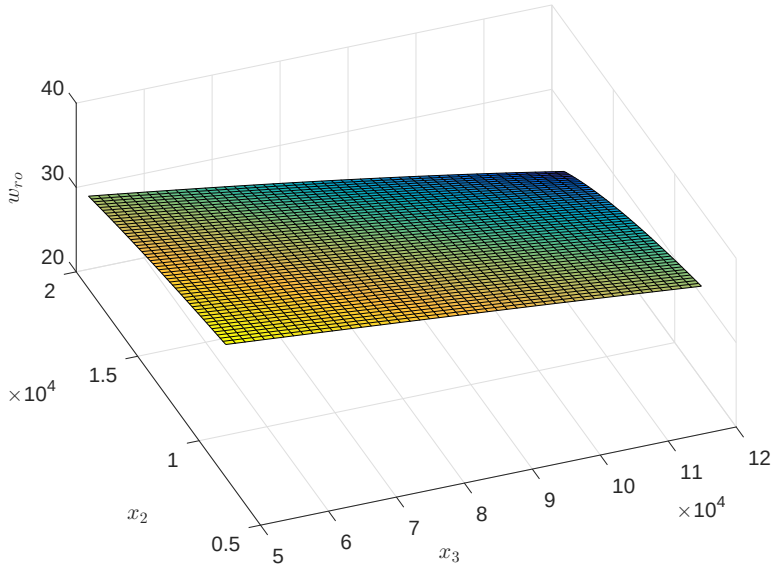

(d) w_{ro} evaluation.

Figure 2.2: Model nonlinear terms evaluation against x_2 and x_3.

2.2.2 Open Loop Step Response (Transient)

The oil production flowrate response (w_{po}) to a gas injection flowrate input step (w_{gc}) ranging from $2kg/s$ to $3kg/s$ is shown in Figure 2.3. It can be seen the transient is very slow and w_{po} only reaches steady state after approximately 4h. Once in steady state it can be observed that output $y = w_{po}$ follows the well performance curve of the system.

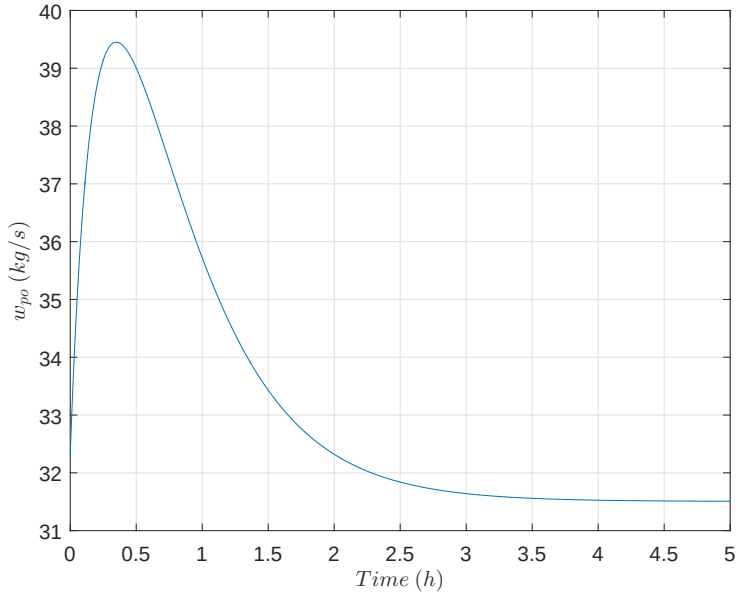

Figure 2.3: The oil production step response: the oil outflow $y = w_{po}$ corresponding to a step in the gas injection flow $u = w_{gc}$ from 2 to 3kg/s.

One can observe that x_1 does not seem to be of much impact on some important variables. In fact, due to the dynamics of x_1, w_{iv} can be considered to be almost equal to w_{gc} and therefore the control input u of the system. Figure 2.4 shows that for a step input of w_{gc}, the time required for w_{iv} stabilize at the same level is approximately 5 times faster than the stabilization of the output w_{po}. Knowing that a step input is not a perfect representation of the gas injection input, a delay ($TF = \frac{1}{10^3 s+1}$) is included to get simulation closer to the reality . In this case can be observed that w_{iv} presents just a small error compared to w_{gc} as shown in Figure 2.5, when the stabilization occurs roughly after an hour . Therefore the conclusion is that w_{iv} can be deemed to be the system input u with no substantial loss of original model dynamics.

2.2.3 Open Loop Step Response and I/O Steady State Mapping

Besides output w_{po} verification, it is crucial to get a deeper knowledge of the system behavior to observe how other variables are impacted by a change in the input $u = w_{gc}$. All charts of Figures 2.6 show steady state curves when the input w_{gc} varies from 1 to 4 kg/s. The output w_{po} from (2.9) can be rewritten as follows dividing both numerator and denominator by x_3:

$$y = w_{po} = \frac{1}{\frac{x_2}{x_3} + 1}\, w_{pc}\,. \tag{2.30}$$

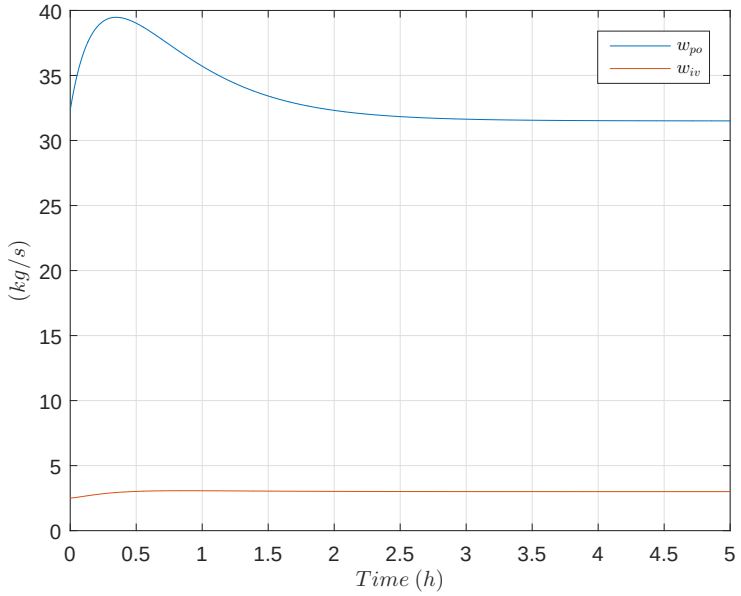

Figure 2.4: w_{iv} and w_{po} settling time comparison.

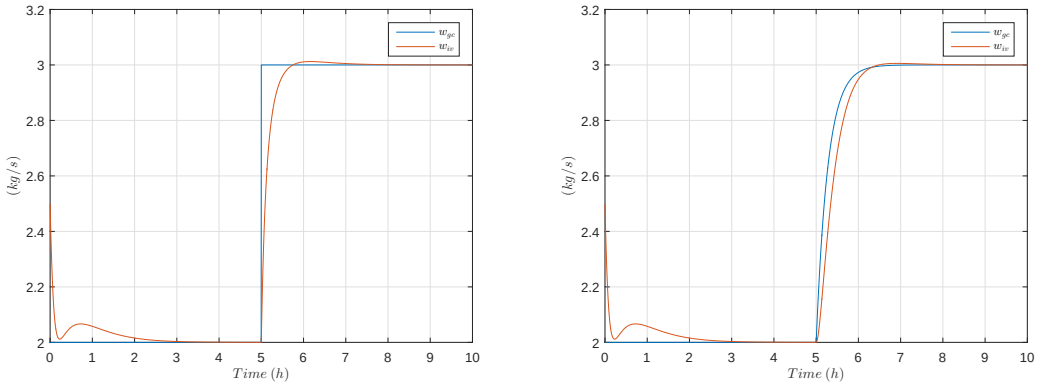

(a) Step input. (b) Smooth input.

Figure 2.5: w_{gc} input step and smooth comparison.

Figure 2.6g shows that w_{pc} is directly proportional to w_{gc}, x_1 and x_2 while x_3 decreases in inverse proportion to them. Looking at (2.30) it can be seen that w_{pc} will get higher if w_{gc} is increased, but the term $\frac{1}{\frac{x_2}{x_3}+1}$ will decrease. The combination of both allows w_{po} to have a peak as shown in Figure 2.6f. The wellhead pressure p_{wh} from (2.16) can be rewritten as:

$$p_{wh} = \frac{\alpha_1 x_2}{\alpha_2 - \alpha_3 x_3}, \tag{2.31}$$

where α_1, α_2 and α_3 are constants defined as follows: $\alpha_1 = \frac{RT_w}{M}$, $\alpha_2 = L_w A_w + L_r A_r$ and $\alpha_3 = v_o$. According to (2.31) and Figures 2.6b, 2.6c, 2.6h it can be observed that p_{wh} gets higher as x_2 increases and x_3 decreases. Density of the mixture ρ_m

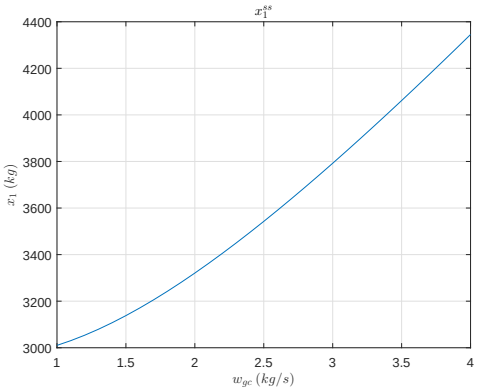

(a) x_1 steady state map.

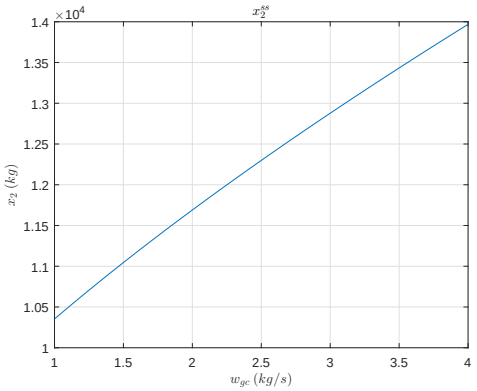

(b) x_2 steady state map.

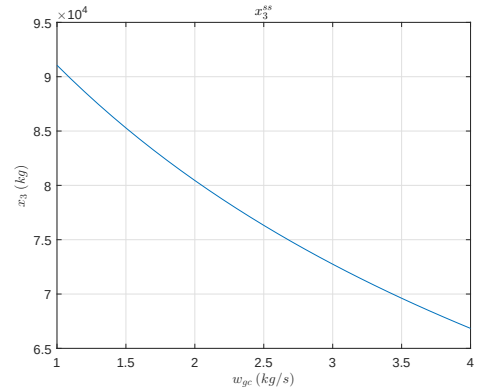

(c) x_3 steady state map.

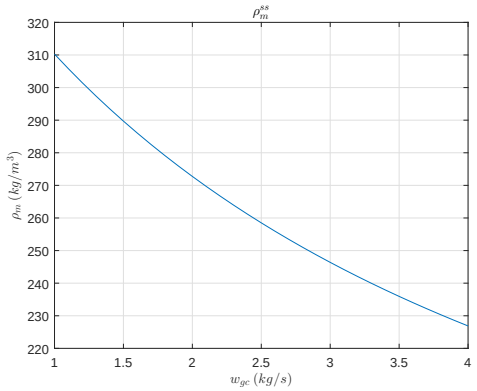

(d) ρ_m steady state map.

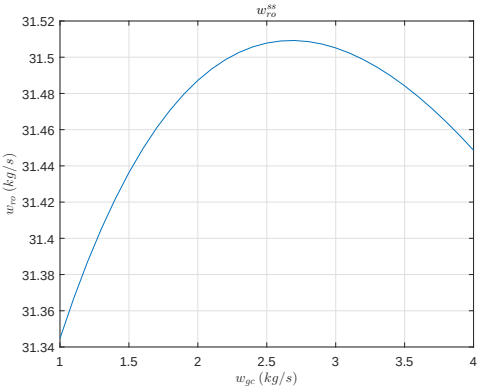

(e) w_{ro} steady state map.

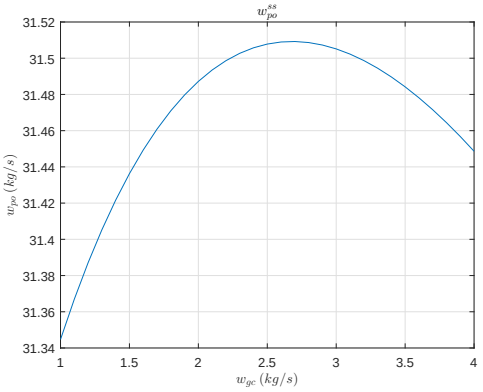

(f) w_{po} steady state map.

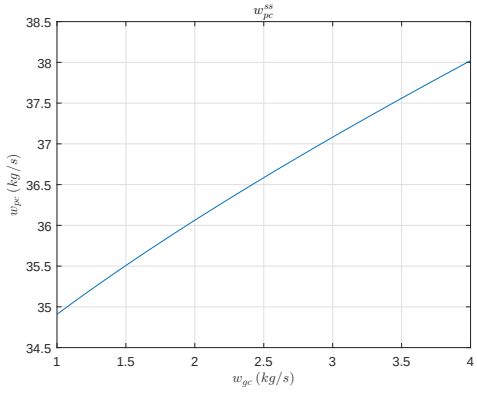

(g) w_{pc} steady state map.

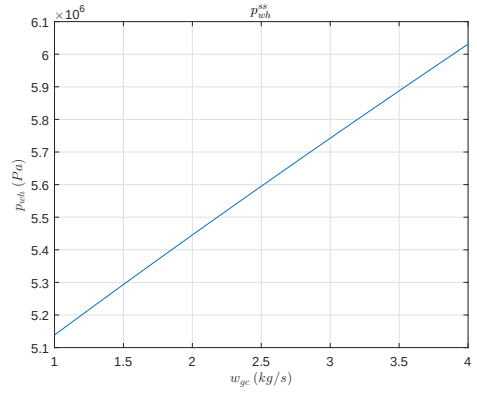

(h) p_{wh} steady state map.

Figure 2.6: System steady state map.

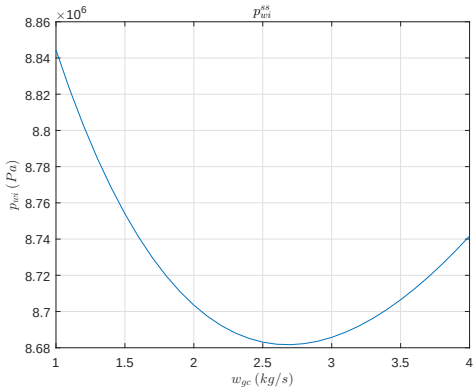

(i) p_{wi} steady state map.

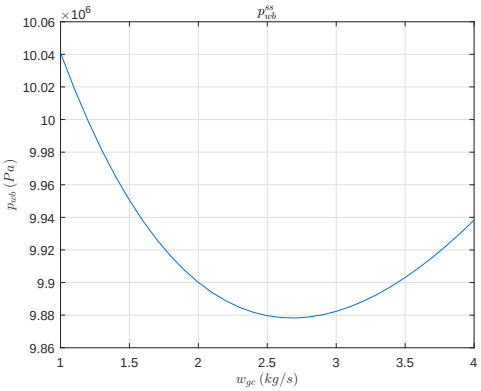

(j) p_{wb} steady state map.

Figure 2.6: System steady state map.

from (2.13) can be rewritten using (2.31) as:

$$\rho_m = \frac{x_2 + x_3 - \alpha_4}{\alpha_5}\,, \tag{2.32}$$

where $\alpha_4 = \rho_o L_r A_r$ and $\alpha_5 = L_w A_w$. Since the absolute value of x_3 is greater than the absolute value of x_2, the difference between them when the first has a negative slope and the second has a positive slope results in a negative slope as shown in Figure 2.6d.

The existence of a static input-output mapping corresponding to (2.29) is described in [5]. In this work the gas flowrate from the reservoir is included in the analysis as follows:

(A0.a) For fixed values of $u(t) = \theta_u \in \mathbb{R}$, the system (2.29) has a unique and constant steady state solution ($\dot{x}_1 = \dot{x}_2 = \dot{x}_3 = 0$), denoted by the equilibrium point $x_1(t) = \theta_1$, $x_2(t) = \theta_2$ and $x_3(t) = \theta_3$ when $t \to +\infty$.

By solving the following algebraic system numerically for some values of θ_u in the region of interest $\theta_u \in [1, 4]$, it can be verified that this assumption **(A0.a)** is not restrictive.

$$\theta_u - \varphi_1(x_1, x_2, x_3) = 0\,, \tag{2.33}$$

$$\varphi_1(x_1, x_2, x_3) + r_{go}\varphi_2(x_2, x_3) - \frac{x_2}{x_3}\varphi_3(x_2, x_3) = 0\,, \tag{2.34}$$

$$\varphi_2(x_2, x_3) - \varphi_3(x_2, x_3) = 0\,. \tag{2.35}$$

For each θ_u, the system (2.33)–(2.35) resulted in a single solution (x_1, x_2, x_3) and, consequently, $y(t)$ converges to a single value in steady state $y(t) = \varphi_3(x_2, x_3)$ when $t \to +\infty$. It is possible to plot the curve $u \times y$ to achieve the WPC curve. This curve represents the oil production in steady state for each value of the constant flow of

gas injection. It is shown in Figure 2.6f and repeated in 2.7 for better visualization.

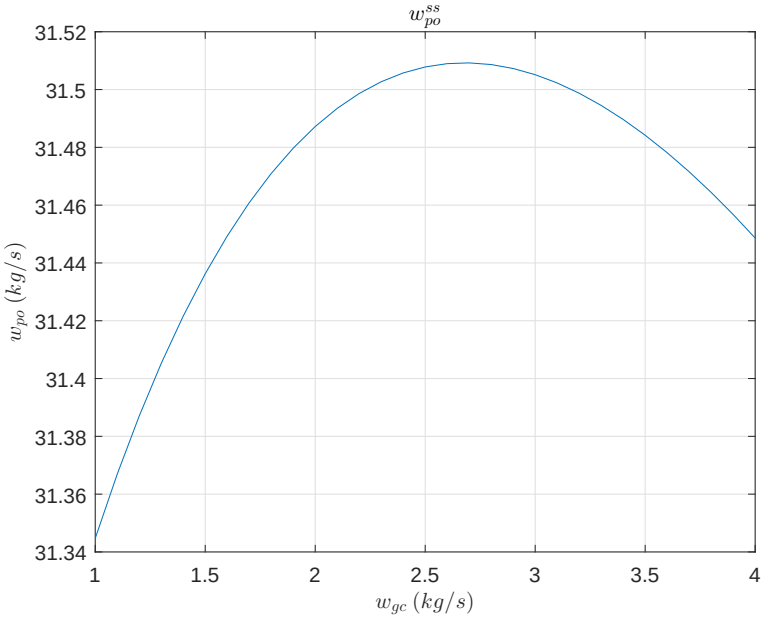

Figure 2.7: The WPC curve: the oil production in steady state $y = w_{po} = \theta_y$ for each value of the gas injection flow $w_{gc} = \theta_u$ in the region of interest $\theta_u \in [1, 4]$.

Figure 2.7 shows that there is a maximum oil flowrate w_{po} is 31.51 kg/s when the gas lift flow is 2.66 kg/s. By examining the solutions (2.33)–(2.35) (an also Figure 2.6) via least squares fitting one can approximate the relationships $x_1(\theta_u)$ and $x_2(\theta_u)$ (increasing functions) and the relationship $x_3(\theta_u)$ (decreasing function). This leads to the following assumption:

(A0.b) There are functions $\alpha_i \in \mathcal{K}_\infty$ $(i = 1, 2)$ and $\beta_3 \in \mathcal{L}$ and constants k_i $(i = 1, 2, 3)$ such that:

$$x_1 = \alpha_1(\theta_u) + k_1, \tag{2.36}$$

$$x_2 = \alpha_2(\theta_u) + k_2, \tag{2.37}$$

$$x_3 = \beta_3(\theta_u) + k_3, \tag{2.38}$$

where $x_1(t)$, $x_2(t)$ and $x_3(t)$ is the unique constant steady state solution of (2.29) corresponding to each fixed value of $u(t) = \theta_u$, according to (A0.a).

From (2.34), the steady state value of the plant output $y = \varphi_3(x_2, x_3)$ is given by

$$y = \varphi_3(x_2, x_3) = \frac{x_3}{x_2}\varphi_1(x_1, x_2, x_3) + r_{go}\varphi_2(x_2, x_3) \tag{2.39}$$

where $\varphi_1(x_1, x_2, x_3)$ is the steady state value of the flow gas $w_{iv} = \varphi_1(x_1, x_2, x_3)$. Moreover, from (2.33), $\varphi_1(x_1, x_{2,3}) = \theta_u$ and from (2.35), $\varphi_2(x_2, x_3) = \varphi_3(x_2, x_3) =$

y, thus one can write

$$y = \frac{x_3}{x_2} \frac{\theta_u}{1 + r_{go}}. \tag{2.40}$$

Finally, from **(A0.b)**, the following input-output relationship at steady state can be obtained:

$$y = \frac{\beta_3(\theta_u) + k_3}{(\alpha_2(\theta_u) + k_2)(1 + r_{go})} \theta_u = \beta(\theta_u)\theta_u \,, \tag{2.41}$$

where $\beta(\theta_u) := \frac{\beta_3(\theta_u)+k_3}{(\alpha_2(\theta_u)+k_2)(1+r_{go})} \in \mathcal{L}$. By using the least squares method, we can obtain α_1, α_2, k_1, k_2, k_3 and β_3.

Knowing that x_2 and x_3 are crucial for many variables of the system a x_2 vs x_3 map may help to better understand system dynamics. Figure 2.8 shows x_2 plotted against x_3. This result was expected and it is in accordance with the curves of Figure

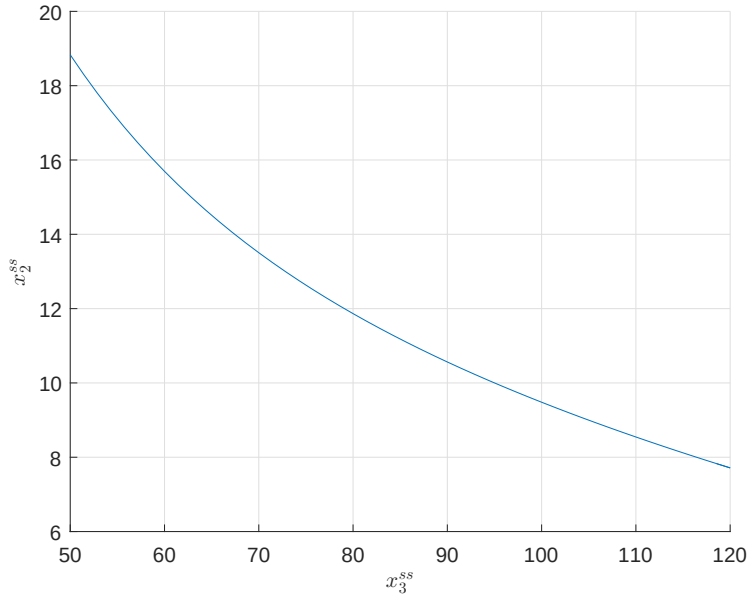

Figure 2.8: x_2 vs x_3 steady state map.

2.6. Additionally it is interesting to understand the output behavior related to the variation of x_2 and x_3. Figure 2.9 shows that both curves have a global maximum.

2.2.4 Open Loop Sinusoidal Response

The steady state response to a sinusoidal input signal is important for a phase difference detection between input and output. According to the classic perturbation-based ESC algorithm this detection is crucial for a good performance of the controller. As can be seen in Figure 2.10 input and output will be in phase if $u < u^*$ and they will be out of phase if $u > u^*$.

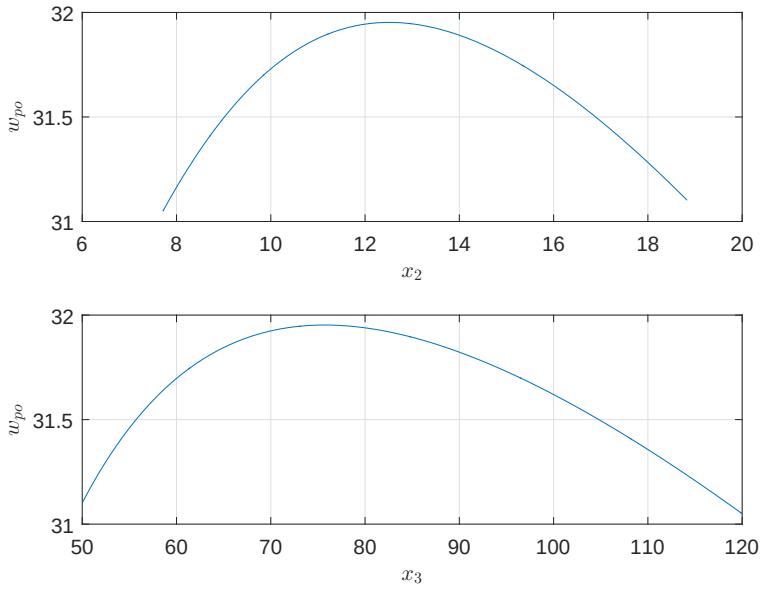

Figure 2.9: x_2 and x_3 vs w_{po}.

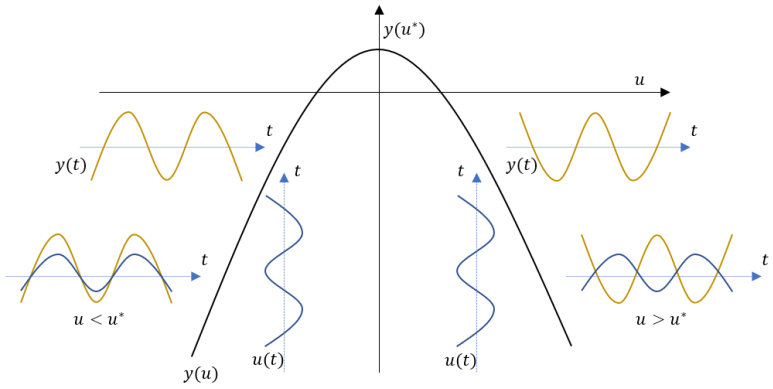

Figure 2.10: Input and output signal behaviour for a suitable perturbation ESC scheme.

The correspondent oil production w_{po} to a sinusoidal gas injection flowrate input of amplitude=0.2 and frequency $\omega = 2\pi/T$, having period $T = 30$ *days* and two different mean values of 2 and 3.8 is shown in Figure 2.11. The aforementioned mean values were evaluated to be the first less then the maximizer and the last greater than the maximizer. It is clear that input and output signals are in phase in Figure 2.11a and out of phase in 2.11b – both signals were adjusted to be in the same scale to aid proper visualization of phase shift. It is clear that the perturbation-based ESC would only work for very low frequencies - similar issue was reported in [5]. Although the proposed model captures the original model dynamics a different ESC scheme needs to be applied for a viable solution. This will be adressed in Chapter 3.2.

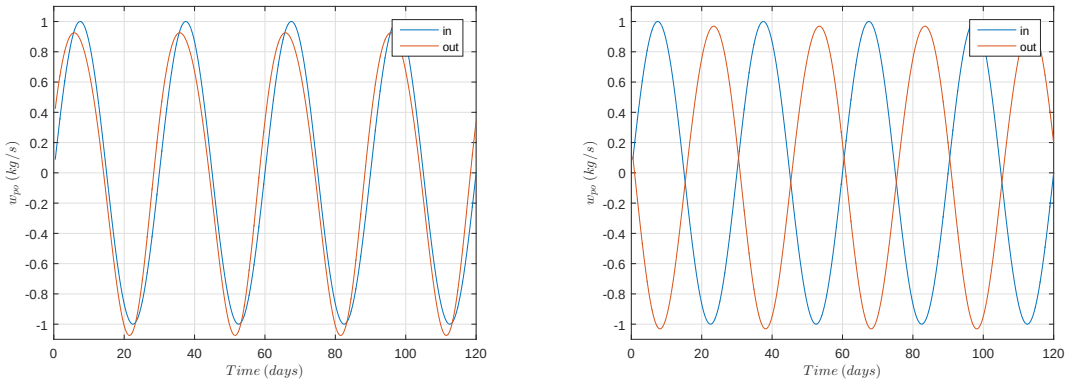

(a) Input and output in phase when $u < u^*$.

(b) Input and output not in phase when $u > u^*$.

Figure 2.11: Plant input and output in steady state. The input and output mean values were removed to clear illustrate the phase shift.

2.3 Model Approximation

From (2.29) and as already observed in [5] the system has three main time scales, repeated here for convenience:

- Fastest – the x_1-dynamics, see also (2.1): the time interval required for the equalization of the gas injection flow in the production column ($w_{iv} = \varphi_1$) and the gas injection flow $u = w_{gc} = \theta_u$, for a constant θ_u.
- Medium – the x_2-dynamics, see also (2.2): the time interval required for the equalization of the gas production flow ($w_{pg} = x_2\varphi_3/x_3$) and the gas injection flow in the production column ($w_{iv} = \varphi_1$), corresponding to a constant $u = w_{gc} = \theta_u$.
- Slow – the x_3-dynamics, see also (2.3): the time interval required for the equalization of the oil production flow ($w_{po} = \varphi_3$) and the oil flow from the reservatoir ($w_{ro} = \varphi_2$), corresponding to a constant $u = w_{gc} = \theta_u$.

A first order model was proposed in [5] taking into account a difference between the system's time constants capturing main features of the Eikrem's model:

- The static input-output relationship described by the WPC curve with maximizer $u^* = w^*_{gc}$ and maximum $y^* = w^*_{po}$.
- A large transient settling time and a large transient peak corresponding to a step input signal.
- Steady state response to a slow sinusoidal input in phase with the input, when the average input level is below the maximizer u^*, and out of phase when the average input level is above u^*.

Since the model obtained at that time was not of the class of Hammerstein-Wienner (HW) systems, compensators had to be added to the ESC scheme so that the period of periodic perturbation could be reduced. The focus of the present work is to find a new way to apply ESC to the modified Eikrem‘s model directly with no need to add additional blocks to the system.

2.3.1 Nonlinear Second Order Modified Eikrem's Model

In Section 2.2.3, it was verified that the w_{iv}-dynamics is the fastest one of the system so that it can be disregarded without affecting the whole system dynamics. Therefore, the control input is given by $u = w_{iv} \simeq w_{gc}$ and the modified Eikrem's Model (a $3^r d$ order model) can be approximated by the following 2^{nd} order nonlinear dynamics:

$$\dot{x}_2 = u + w_{rg} - w_{pg}\,, \tag{2.42}$$

$$\dot{x}_3 = w_{ro} - w_{po}\,, \tag{2.43}$$

$$y = w_{po}\,. \tag{2.44}$$

This approximations can be further justified by comparing the open loop step response for the 3^{rd} and 2^{nd} modified Eikrem's Model as illustrated in Figure 2.12, where it is evident that both step responses are similar. By reminding that $w_{pg} = \frac{x_2}{x_3} w_{po} = \frac{x_2}{x_3} y$, $w_{rg} = r_{go} w_{ro}$ and w_{rg} and w_{po} are nonlinear functions depending only on x_2 and x_3, then (2.42)–(2.44) can be rewritten as:

$$\dot{x}_2 = u + r_{go} w_{ro}(x_2, x_3) - \frac{x_2}{x_3} y\,, \tag{2.45}$$

$$\dot{x}_3 = w_{ro}(x_2, x_3) - y\,, \tag{2.46}$$

$$y = w_{po}(x_2, x_3)\,. \tag{2.47}$$

It is worth mentioning the comments in Section 2.2.3, regarding the 1^{st} dynamic approximation also apply here, i.e., the proposed 2^{nd} order model also captures the following main features of the 3^{rd} order modified Eikrem's model, repeated here for convenience:

- The static input-output relationship described by the WPC curve with maximizer $u^* = w_{gc}^*$ and maximum $y^* = w_{po}^*$.
- A large transient settling time and a large transient peak corresponding to a step input signal.
- Steady state response to a slow sinusoidal input in phase with the input, when the average input level is below the maximizer u^*, and out of phase when the

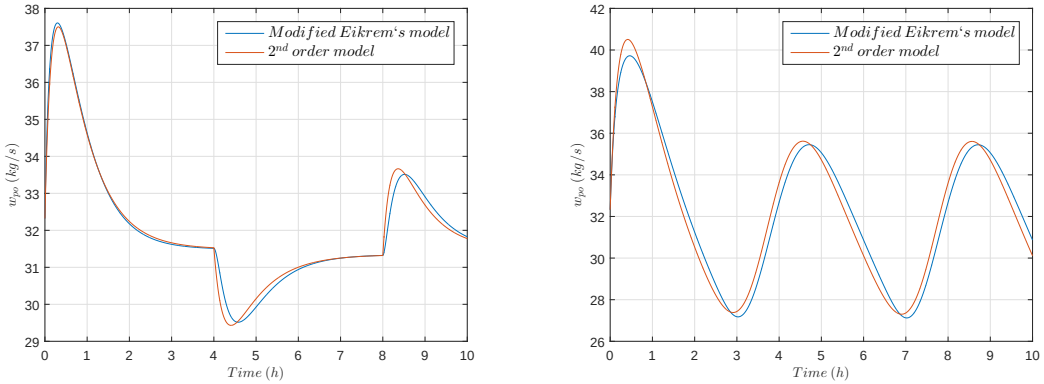

(a) Step response.

(b) Sinusoidal response.

Figure 2.12: Model validation: comparison between the modified Eikrem model and the 2^{nd} order models.

average input level is above u^*.

2.3.2 Partial Linearized Second Order Eikrem's Model

According to Section 2.2.1, where all nonlinear functions were evaluated, one can verify in particular that nonlinear term $w_{ro}(x_2, x_3)$ can be approximated by a linear function in x_2 and x_3. In fact, the following approximation can be obtained via least square:

$$w_{ro}(x_2, x_3) \approx c_1 x_2 + c_2 x_3 + c_3 \,, \tag{2.48}$$

where c_1, c_2 and c_3 are constants. From Figure 2.2d, one can observe that the oil flow rate from the reservoir to the tubing w_{ro} can in fact be approximated by a linear function of x_2 and x_3.

Considering this linear approximation, the 2^{nd} order model (2.42)–(2.44) can be approximated by:

$$\dot{x}_2 = u + r_{go}[c_1 x_2 + c_2 x_3 + c_3] - \frac{x_2}{x_3} y \,, \tag{2.49}$$

$$\dot{x}_3 = [c_1 x_2 + c_2 x_3 + c_3] - y \,, \tag{2.50}$$

$$y = w_{po}(x_2, x_3) \,, \tag{2.51}$$

which will be useful for control design. However, it must be highligthed that this approximation also captures the main features of the 3^{rd} order Eikrem's model mentioned before.

Chapter 3

Inner and Outer Loops

In this chapter, the closed inner loop control is employed to accelerate the closed loop dynamics before applying ESC scheme in the outer loop, when the optimization problem is then addressed.

3.1 Inner Loop: Tracking Control

The objective of oil production optimization in gas lift oil wells is to drive the gas lift to maximize production while keeping it around the maximum value of the WPC curve.

In what follows, it is put in evidence the main available subsea instruments that can be used for state estimation of the Eikrem's model, giving support to development of an inner tracking controller.

3.1.1 Subsea Instrumentation

Since the 1980s multiplexed electro-hydraulic control systems have been employed in subsea oil and gas production [67]. Subsea sensors have always played a critical role in a successful operation of an offshore production unit. Originally analog, they were very prone to different kinds of failures and external interference which compromised instruments reliability. Nowadays digital options are available when the environment is not suitable for analogical sensors. In 2003 the Subsea Instrumentation Interface Standardisation (SIIS) was established with a remit to create an open standard for the benefit of oil and gas industry as a whole [68].

SIIS has produced a Recommended Practice (RP) and text for an API Standard defining three instrument interface protocols for communication between Subsea Control Modules (SCM) and subsea sensors:

- Level 1: Analogue Devices: These devices are 4-20mA sensors, 2 wire loop powered analogue output sensing devices.

- Level 2: Digital Serial Devices (CANopen).
- Level 3: Ethernet TCP-IP Devices.

Developments on subsea instrumentation has led to rapidly spread of digital sensors based on SIIS level 2 and 3 specifications, besides level 1 already broadly used by the industry. The main advantages of digital sensors consist in possible count on fault tolerant and dual redundant devices but still having fast update rates up to several readings per second. Just to mention a few examples, CANopen fault tolerant instruments can provide reliable data even if there is a wire break or a short in some of the power wires. A pressure transmitter can still work on secondary electronics if the primary electronics or a sensor element fails for any reason.

Likewise, the Intelligent Well Interface Standardisation (IWIS) has produced a RP for interface with downhole equipment, including standards to be followed, communications systems, memory allocation and acceptance tests [69]. The immediate consequence is having more reliable transmitters and data readings from downhole sensors also know as Permanent Downhole Gauge (PDG) . This means that is no longer necessary to estimate downhole pressure and temperature as can be found in literature. A possible Wet Christmas Tree (WCT) diagram is shown in Figure 3.1.

Subsea systems are constantly evolving and the introduction of electrical actuators has enabled the rise of "all electric" systems – marine electrical motors for valve actuation can replace hydraulic systems and their requirement of multiple flying leads and fluid cleanliness high standards. This is constantly understood as a way for more cost effective systems. Although this subject will not be approached in the present, some reference can be found in [70] and [71].

As can be seen in Figure 3.1 several data values are available, from pressure and temperature transmitters, as listed in Table 3.1. It is very usual to have pressure and

Table 3.1: WCT available sensors

Instrument	**Model Variables**	**Description**
PTT 1	p_s	Pressure downstream PMV
PTT 5	p_{wh}	Pressure upstream PMV
PDG	p_{wb}, p_{wi}	Pressure at bottom of tubing and at injection port
WGFM	w_{gc}	Gas lift flow rate
MPFM	w_{pc}, w_{pg}, w_{po}	Production flow rate
PTT 3	n/a	Anular pressure and temperature

instruments located at master and annulus bores of a WCT. Therefore Pressure and Temperature Transmitter *PTT 1* readings could be used as p_s if it was not deemed constant in this work. Although not typical, a *PTT 5* located upstream *PMV* will be

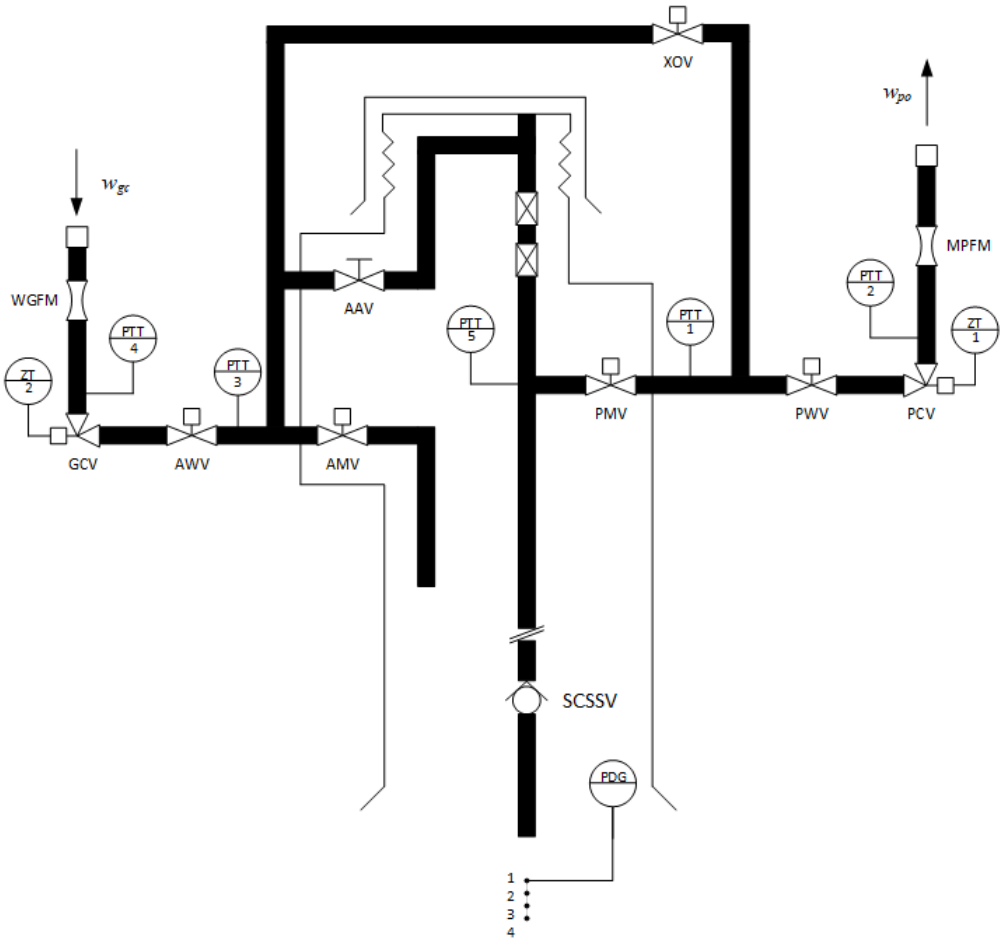

Figure 3.1: WCT instrumentation illustration.

considered in this work to serve as p_{wh}. The existence of downhole gauges can provide readings for p_{wb} and p_{wi}. Although there is no variable in the model for pressure at the top of annular, *PTT 3* could be used to estimate p_{ai}. A Wet Gas Flowmeter *WGFM* can be directly related to the input w_{gc} - it cannot control the flow rate but confirms it is according to the desired value. A Multiphase Flowmeter *MPFM* is a more complex instrument which usually is installed in retrievable structures to be used in different wells only when necessary. Despite its limited availability it can provide flow rates readings of production - oil and water flow rates (w_{po}) and gas flow rates (w_{pg}) in real time, becoming very valuable for a closed loop feedback control. The assumptions that p_{wh} and p_{wi} are available represents a new approach to the gas lifted oil wells optimization problem enabling new observers based on state estimation of the system.

It is worth mentioning that several simplifications are in place for the development of the control of this work. Regarding the gas lift injection, while it is been considered only one point of injection at the bottom of the tubing, currently it is possible to inject gas at reservoir level, bypassing the packer. Although pressure downstream p_s production choke and reservoir pressure p_r is deemed constant in the

present work, the first is constantly monitored as show in Figure 3.1 and the second can also be monitored with commercial equipment.

Table 3.2 shows all parameters highlighting which can be considered known or unknown, as well as, all signal that are available or not for feedback, depending on the process instrumentation.

Table 3.2: Availability of Model Parameters and Signals

Parameters	**Availability**	**Comments**
T_a	Uncertain	Estimated via TT
L_a	Known	from Tubing Mechanical Design
V_a	Known	from Tubing Mechanical Design
A_r	Known	from Tubing Mechanical Design
A_w	Known	from Tubing Mechanical Design
C_{iv}	Known	from Valve Mechanical Design
C_{pc}	Known	from Choke Mechanical Design
C_r	Uncertain	Considered not easily measured or estimated
g	Known	Gravity Acceleration
L_r	Known	from Tubing Mechanical Design
L_w	Known	from Tubing Mechanical Design
M	Known	Gas properties are known
μ	Uncertain	Viscosity of the fluid (periodically evaluated)
R	Known	Universal gas constant
r_{go}	Uncertain	Estimated by production of oil and gas
ρ_o	Known	Oil properties are known
T_w	Uncertain	Estimated via TT
Signals	**Availability**	**Comments**
p_r, p_{wb}, p_{wi}	Available	via (PDG)
p_s, p_{wh}	Available	via Pressure Transmitters (PT)
ρ_m	Not Available	Oil and gas properties
w_{pc},w_{pg},w_{po}	Available	via Multiphase Flowmeter (MPFM)
w_{ro},w_{rg}	Not Available	Oil and gas plus tubing properties

3.1.2 Possible Scenarios

In what follows, it is formulated a set of assumptions and corresponding dynamic models used for control design, depending on the availability of parameters/signals illustrated in Table 3.2. In particular, the oil flow rate from the reservoir to the tube w_{ro} plays an important role: it can be treated as an uncertain/certain nonlinear/linear function of the plant states x_2 and x_3, or as an available exogenous signal (possibly *modulo* an uncertain gain).

First Scenario

It is clear that, when x_2 and x_3 are available for feedback and all parameters are known, all signals are available and feedback linearization can be employed for tracking. The following assumption reflects this ideal condition.

(A1.a) The parameters r_{go}, ρ_o, p_r, g, L_r, A_w, A_r, R, M and L_w are known.

(A1.b) The plant states x_2 and x_3 and the output y are available for feedback.

(A1.c) The parameters C_r and T_w are known.

Assumption **(A1.a)** is not restrictive since all those parameter can be obtained or estimated, as described in Table 3.2. In particular, the parameter r_{go} can be obtained via experiments in steady state. Indeed, by denoting w_{rg}^{ss} as the steady state value of w_{rg}, one can write:

$$w_{rg}^{ss} = w_{pg}^{ss} - w_{iv}^{ss}\,,$$

where w_{pg}^{ss} and $w_{iv}^{ss} = u^{ss}$ are also steady state values. Therefore, reminding that $w_{rg} = r_{go}w_{ro}$ and $w_{ro}^{ss} = w_{po}^{ss} = y^{ss}$, then the constant r_{go} can be estimated by:

$$r_{go} = \frac{w_{pg}^{ss} - u^{ss}}{y^{ss}}\,,$$

since w_{pg} is available for feedback via a MPFM. However, Assumption **(A1.c)** represents a restriction of the following control design. This can be relaxed by using a robust control scheme.

Assumption **(A1.b)** can be relaxed by using the static estimates for x_2 and x_3 provided in Section 3.1.3. Note that, those estimates can be deteriorated by parameter variation and/or measurement noise. Thus, dynamic observers should be designed.

Under Assumption **(A1)**, a linearized approximation of the term $w_{ro}(x_2, x_3) = c_1x_2 + c_2x_3 + c_3$ can be obtained, with **known** constants c_1, c_2 and c_3. So, as mentioned in Chapter 2, the 2^{nd} order model (2.49)–(2.51) is used for control design. This model is repeated in the following for convenience:

$$\dot{x}_2 = u + r_{go}[c_1x_2 + c_2x_3 + c_3] - \frac{x_2}{x_3}y\,, \tag{3.1}$$

$$\dot{x}_3 = [c_1x_2 + c_2x_3 + c_3] - y\,, \tag{3.2}$$

$$y = w_{po}(x_2, x_3)\,. \tag{3.3}$$

For simplicity, as a preliminary design, it is considered that the parameters are known as in **(A1.a)** and **(A1.c)** so that a feedback linearization control can be

applied, with or without state estimation. However, output feedback robust control schemes can also be considered for relaxing this parameter assumptions.

The feedback linearization controller, under the assumption of perfect knowledge of the plant, is given by:

$$u := \frac{x_2}{x_3} y - r_{go}[c_1 x_2 + c_2 x_3 + c_3] + K_2(x_2^d - x_2)\,, \tag{3.4}$$

$$c_1 x_2^d := -[c_2 x_3 + c_3] + y + K_3(x_3^d - x_3) + \dot{x}_3^d\,, \tag{3.5}$$

where x_3^d is the desired trajectory for x_3 and K_2, K_3 are design constants. Thus, the closed loop system is written as

$$\dot{x}_2 = K_2(x_2^d - x_2)\,, \tag{3.6}$$

$$\dot{x}_3 = [c_1 x_2 + c_2 x_3 + c_3] - y\,, \tag{3.7}$$

$$y = w_{po}(x_2, x_3)\,. \tag{3.8}$$

One alternative is to incorporate the time derivative of the desired trajectory x_2^d for x_2 in the control signal u in (3.4), as a feedforward action. However, the time derivative $\dot{y}$ or (at least) an estimate for $\dot{y}$ is required. In this case, the control effort is redefined as:

$$u := \frac{x_2}{x_3} y - r_{go}[c_1 x_2 + c_2 x_3 + c_3] + K_2(x_2^d - x_2) + \dot{x}_2^d\,, \tag{3.9}$$

$$c_1 x_2^d := -[c_2 x_3 + c_3] + y + K_3(x_3^d - x_3) + \dot{x}_3^d\,, \tag{3.10}$$

$$c_1 \dot{x}_2^d := -[c_2 \dot{x}_3 + c_3] + \dot{y} + K_3(\dot{x}_3^d - \dot{x}_3) + \ddot{x}_3^d\,, \tag{3.11}$$

where $\dot{x}_3 = [c_1 x_2 + c_2 x_3 + c_3] - y$ depends only on x_2, x_3 and y. Thus, the closed loop system is written as

$$\dot{x}_2 = K_2(x_2^d - x_2) + \dot{x}_2^d\,, \tag{3.12}$$

$$\dot{x}_3 = [c_1 x_2 + c_2 x_3 + c_3] - y\,, \tag{3.13}$$

$$y = w_{po}(x_2, x_3)\,. \tag{3.14}$$

Note that, in order to implement the control law (3.9)–(3.11), the constants c_1, c_2, c_3, r_{go} must be known and the signals $x_2, x_3, \dot{y}$ and the desired trajectory for x_3^d and its time derivatives $\dot{x}_3^d$ and $\ddot{x}_3^d$. It must be highlighted that state estimates can be used replacing the actual ones. Moreover, robust tracking controller can used when the plant parameters are uncertain.

The constants c_1, c_2, c_3, r_{go} can be obtained if **(A1.a)** holds. However, this assumption can be relaxed by considering the next scenario.

Second Scenario

Now, consider the following assumptions:

(A2.a) The parameter p_r is known.

(A2.b) The plant states x_2 and x_3 and the signal p_{wb} are available for feedback.

Assumption **(A2)** assures that the oil flow rate from the reservoir to the tube w_{ro} is an available signal $w_{ro} = C_r\sqrt{\rho_o}\sqrt{p_r - p_{wh}}$, *modulo* the unknown multiplying constant $C_r\sqrt{\rho_o}$. Moreover, from the 2^{rd} order model (2.49)–(2.51), one has:

$$w_{ro} = C_r\sqrt{\rho_o}\underbrace{\sqrt{p_r - p_{wh}}}_{\mu_{ro}} = [c_1x_2 + c_2x_3 + c_3]\,, \tag{3.15}$$

and, for this case, the following model is considered for control design:

$$\begin{aligned}
\dot{x}_2 &= u + r_{go}C_r\sqrt{\rho_o}\mu_{ro} - \frac{x_2}{x_3}y\,, &(3.16)\\
\dot{x}_3 &= \underbrace{[c_1x_2 + c_2x_3 + c_3]}_{=C_r\sqrt{\rho_o}\mu_{ro}} - y\,, &(3.17)\\
y &= w_{po}(x_2, x_3)\,, &(3.18)
\end{aligned}$$

where $\mu_{ro} := \sqrt{p_r - p_{wh}}$ $(p_r > p_{wb})$. The control effort is redefined as:

$$\begin{aligned}
u &:= \frac{x_2}{x_3}y - r_{go}C_r\sqrt{\rho_o}\mu_{ro} + K_2(x_2^d - x_2) + \dot{x}_2^d\,, &(3.19)\\
c_1x_2^d &:= -[c_2x_3 + c_3] + y + K_3(x_3^d - x_3) + \dot{x}_3^d\,, &(3.20)\\
c_1\dot{x}_2^d &:= -[c_2\dot{x}_3 + c_3] + \dot{y} + K_3(\dot{x}_3^d - \dot{x}_3) + \ddot{x}_3^d\,, &(3.21)
\end{aligned}$$

where $\dot{x}_3 = C_r\sqrt{\rho_o}\mu_{ro} - y$ depends only on μ_{ro} and y.

Note that, in order to implement the control law (3.19)–(3.21), the constants $c_1, c_2, c_3, r_{go}, C_r$ and ρ_o must be known and the signals $x_2, x_3, \dot{y}$ and the desired trajectory for x_3^d and its time derivatives $\dot{x}_3^d$ and $\ddot{x}_3^d$.

Now, consider the following assumption:

(A2.c) The parameters r_{go}, ρ_o and C_r are known.

Under this Assumption **(A2.c)**, the oil flow rate from the reservoir to the tube w_{ro} becomes a complete available signal and can be compensated via feedback linearization. In addition, constants c_1, c_2, c_3 can be obtained via least squares by using (3.15). When ρ_o is considered uncertain, robust control strategies could be applied for tracking and, as mentioned before, Assumption **(A2.b)** can be relaxed by using the static estimates given in Section 3.1.3. Remind that those estimates can be deteriorated by parameter variation and/or measurement noise. Thus, dynamic observers should be designed.

3.1.3 Plant State Estimation

The model presented in Chapter 2 relies on masses of gas and oil in the annular and production tubing. Typically there is no sensors for such data, however state estimate sounds reasonable by using the available signals described in Table 3.2.

Indeed, from (2.9) the following can be obtained:

$$\frac{x_3}{x_2 + x_3} = \frac{w_{po}}{w_{pc}}\,, \tag{3.22}$$

$$\frac{x_3}{x_2} = \frac{w_{po}}{w_{pc} - w_{po}} = \frac{y}{w_{pc} - y} := \mu_1\,, \tag{3.23}$$

where μ_1 is an available signal obtained by using $y = w_{po}$ and w_{pc} via a MPFM. Hence, the ratio $\mu_1 = x_3/x_2$ is known.

From (2.22), the following can be obtained:

$$w_{pc}^2 = C_{pc}^2 \rho_m (p_{wb} - p_s)\,, \tag{3.24}$$

provided $p_{wb} > p_s$ and $u_c = 1$. Therefore, the unavailable signal ρ_m can be estimated by

$$\rho_m = \frac{w_{pc}^2}{C_{pc}^2 (p_{wb} - p_s)}\,,$$

where p_{wb}, p_s are measured via PDG and w_{pc} via a MPFM.

In addition, from (2.13) one can write

$$x_2 + x_3 = \rho_m L_w A_w + \rho_o L_r A_r\,, \tag{3.25}$$

or, equivalently,

$$x_2 + x_3 = L_w A_w \frac{w_{pc}^2}{C_{pc}^2 (p_{wb} - p_s)} + \rho_o L_r A_r := \mu_2\,. \tag{3.26}$$

It means that the sum $x_2 + x_3 = \mu_2$ is known. Finally, the states x_2 and x_3 can be obtained via the following estimates:

$$\hat{x}_2 = \frac{\mu_2}{\mu_1 + 1}\,, \tag{3.27}$$

$$\hat{x}_3 = \frac{\mu_1 \mu_2}{\mu_1 + 1}\,. \tag{3.28}$$

In summary, the following assumption is needed to obtain the estimates (3.27)–(3.28):

(A3.a) The parameters ρ_o, L_r, A_r, C_{pc}, L_w and A_w are known.

(A3.b) The signals y, w_{pc}, p_{wb} and p_s are available for feedback.

Assumption (**A3.a**) is reasonable to hold, as described in Table 3.2. Assumption **(A3.b)** is not restrictive when a MPFM, a PDG and a PT are employed in the oil well architecture. Moreover, in (**A3.b**), one can also assume that w_{pg} is measured while w_{pc} is estimate via $w_{pc} = w_{pg} + y$.

As an alternative, one can obtain the state estimates without using the w_{pc} measurement. In fact, by using only pressure measurements the plant state can be estimated in what follows.

From (2.16), one has that

$$x_2 = \underbrace{p_{wh}\frac{M}{RT_w}(L_w A_w + L_r A_r)}_{:=\mu_3} - \underbrace{p_{wh}\frac{M}{RT_w}v_o}_{:=\mu_4} x_3 \,,$$

and from (2.17) one can write:

$$x_2 + x_3 = (p_{wi} - p_{wh})\frac{A_w}{g} + \rho_o L_r A_r := \mu_5 \,.$$

Then, the states satisfy

$$x_2 + \mu_4 x_3 = \mu_3 \quad \text{and} \quad x_2 + x_3 = \mu_5 \,,$$

where μ_3, μ_4 and μ_5 are available signals and the estimates are given by:

$$\hat{x}_3 = \frac{\mu_3 - \mu_5}{\mu_4 - 1} \,, \tag{3.29}$$

$$\hat{x}_2 = \mu_5 - \hat{x}_3 \,. \tag{3.30}$$

In summary, the following assumption is needed to obtain the estimates (3.30)–(3.29):

(A4.a) The parameters g, M, R, ρ_o, L_r, A_r, L_w and A_w are known.

(A4.b) The pressure signals p_{wh} and p_{wi} are available for feedback.

(A4.c) The parameter T_w is known.

Assumption (**A4.b**) is not restrictive when a PDG and a PT are employed in the oil well architecture. While Assumption (**A4.a**) is reasonable to hold, Assumption **(A4.c)** represents a restriction which can be relaxed in the future by using robust control schemes.

Remark 1. *Note that, if it is considered that the signals p_{wh}, p_{wi}, y, w_{pc} are available*

for feedback, then one can compose those estimates to obtain new estimates via

$$\frac{x_3}{x_2} = \frac{w_{po}}{w_{pc} - w_{po}} = \frac{y}{w_{pc} - y} := \mu_1 \,, \tag{3.31}$$

$$x_2 + x_3 = (p_{wi} - p_{wh})\frac{A_w}{g} + \rho_o L_r A_r := \mu_5 \,. \tag{3.32}$$

provided that A_w, g, L_r, A_r and ρ_o are known. Note that, in this case, there is only one critical parameter (ρ_o).

Remark 2. *The sensibility analysis w.r.t. parameter variation must be performed. For the first estimate methodology, the key parameters for which the sensibility analysis must be carried out are the oil density ρ_o and the flow capacity C_{pc} of the choke. However, the flow capacity can be assumed constant since, in general, the production choke displacement remains fixed during the operation. For the second estimate methodology, the key parameters are T_w and M, ρ_o. If the sensibility is too high, a robust linear/nonlinear dynamic observer must be designed.*

Sliding Mode State Estimator

Note that, if it is considered that the signals p_{wh}, p_{wi}, y, w_{pc} are available for feedback, then one can define the following available parameter free signals:

$$\mu_1 := \frac{y}{w_{pc} - y} \,, \tag{3.33}$$

$$\mu_6 := p_{wi} - p_{wh} \,. \tag{3.34}$$

It is clear that the ratio $\frac{x_3}{x_2} = \frac{w_{po}}{w_{pc}-w_{po}} = \frac{y}{w_{pc}-y} = \mu_1$ is available. Moreover, the signal μ_6 is afine related with the states x_2 and x_3:

$$\mu_6 = \frac{g}{A_w}x_2 + \frac{g}{A_w}x_3 - \rho_o L_r A_r \frac{g}{A_w} = C_0 x + \delta \,,$$

where $x = \begin{bmatrix} x_2 & x_3 \end{bmatrix}^T$, $C_0 = \frac{g}{A_w}\begin{bmatrix} 1 & 1 \end{bmatrix}$ and $\delta := -\rho_o L_r A_r \frac{g}{A_w}$. Now, by using the change of coordinates $w_1 := \mu_6 = C_0 x + \delta$ and $w_2 := x_3$, the system (3.1)–(3.2) can be rewritten as

$$\dot{w} = A_n w + B_n u + \mu_n + D_n + [\tilde{D} + \tilde{A}w] \,, \tag{3.35}$$

$$\mu_6 = C_n w \,, \tag{3.36}$$

where $C_n = \begin{bmatrix} 1 & 0 \end{bmatrix}$, $\mu_n := \begin{bmatrix} -yx_2/x_3 - y & -y \end{bmatrix}^T$, $D_n = \begin{bmatrix} (r_{go}^n + 1)(c_3^n - c_1^n\delta^n) & c_3^n - c_1^n\delta^n \end{bmatrix}^T$, $D = D_n - \begin{bmatrix} (r_{go} + 1)(c_3 - c_1\delta) & c_3 - c_1\delta \end{bmatrix}^T$,

$$B_n = \left[\begin{array}{cc} 1 & 0 \end{array} \right]^T$$

$$A_n = \left[\begin{array}{cc} (r_{go}^n + 1)c_1^n & (r_{go}^n + 1)(c_2^n - c_1^n) \\ c_1^n & c_2^n - c_1^n \end{array} \right]^T ,$$

$$\tilde{A} = A_n - \left[\begin{array}{cc} (r_{go} + 1)c_1 & (r_{go} + 1)(c_2 - c_1) \\ c_1 & c_2 - c_1 \end{array} \right]^T .$$

The following sliding mode observer is employed:

$$\dot{\hat{w}} = A_n\hat{w} + B_nu + \mu_n + D_n - L(C_n\hat{w} - \mu_6) + P^{-1}C_n^T u_s \,, \tag{3.37}$$

where $u_s := -\varrho \text{sgn} C_n\tilde{w}$ and $P = P^T > 0$ is a matrix which satisfies $A_n^T P + PA_n < 0$ and $PB_n = C_n^T$. Such a matrix exists if (A_n, B_n, C_n) is SPR. Otherwise, there exists k_0 such that $(\bar{A}_n, B_n, C_n)$ is SPR, with $\bar{A}_n := A_n - B_nC_nk_0$. In this case, the system and the observer are rewritten as:

$$\dot{w} = \bar{A}_nw + B_nu + \mu_n + D_n + [\tilde{D} + \tilde{A}w + B_nC_nk_0w] \,, \tag{3.38}$$

$$\mu_6 = C_nw \,, \tag{3.39}$$

and

$$\dot{\hat{w}} = \bar{A}_n\hat{w} + B_nu + \mu_n + D_n - L(C_n\hat{w} - \mu_6) + P^{-1}C_n^T u_s \,, \tag{3.40}$$

respectively.

3.1.4 Numerical Simulations

Numeric simulation results proving the efficiency of the proposed controllers are presented in what follows.

The plant parameters are: $c_1 = -5.637 \times 10^{-4}$, $c_2 = -9.266 \times 10^{-5}$, $c_3 = 45.92$, $\rho_o = 923.9$, $C_r = 2.623 \times 10^{-4}$ and $r_{go} = 0.0818$. The control gains are: $K_2 = 0.025$ and $K_3 = 0.001$. The desired trajectory for the oil mass in the tubbing (x_r^d) is given by a stepwise function.

The step response of the closed loop system can be observed in Figure 3.2, for the Eikrem's model and its second order approximation. In Figure 3.3, one can see the mass of gas in the tubbing increasing as x_3^d decreases. Note that overshoot appears due to the abrupt transition of the reference x_3^d and the high gain K_2. The corresponding time history of the gas injection control effort (w_{iv}) is given in Figure 3.4. The transient and steady state of the oil production is illustrated in Figure 3.5.

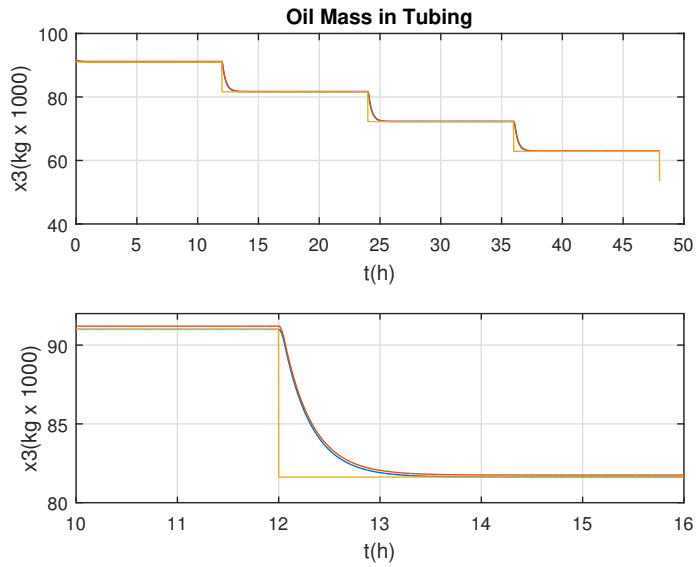

Figure 3.2: The mass of oil in the tubbing.

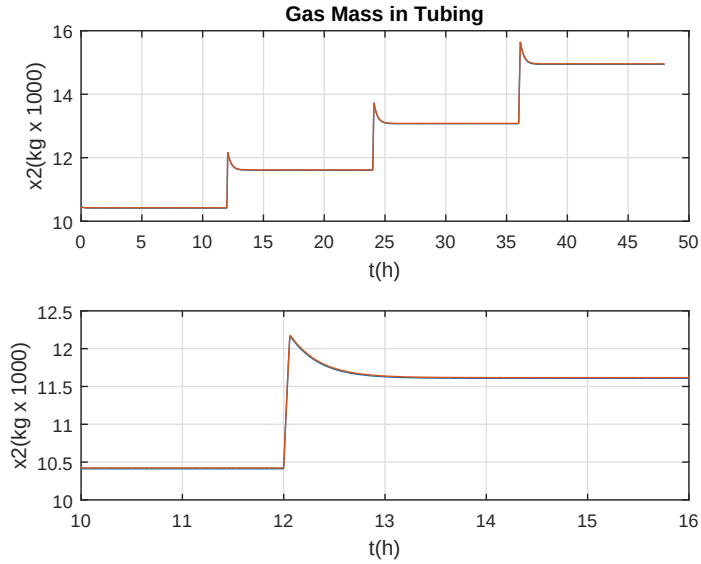

Figure 3.3: The mass of gas in the tubbing.

3.2 Outer Loop: Extremum Seeking Control

This section aims to provide control algorithms based on Extremum Seeking Control so that the Well Performance Curve is maximized on line. Hence, at first, a background on ESC is provided along with some of the algorithm's usual applications and major benefits. Finally, the simulation is performed to illustrate the ESC results.

According to [72], one can say that "Extremum seeking control is a non-model based real-time optimization approach for dynamic problems where only limited knowledge of a system is available, such as when the system has a nonlinear equilibrium map which has a local minimum or maximum". The main methods

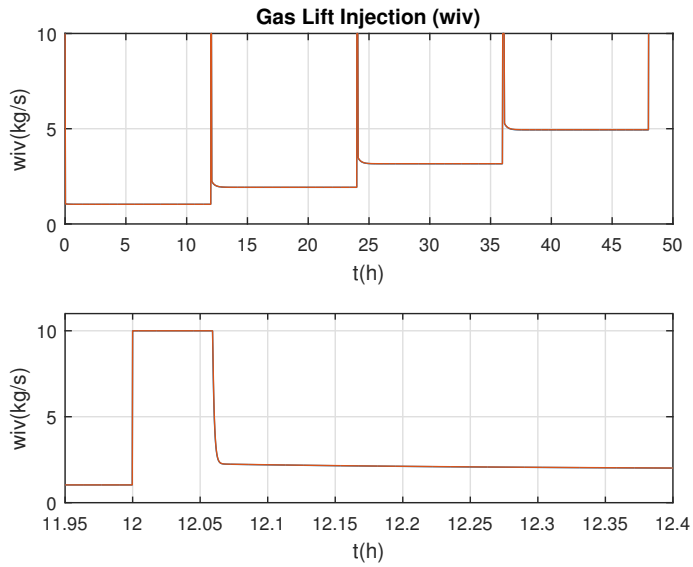

Figure 3.4: The control effort w_{iv}: gas injection.

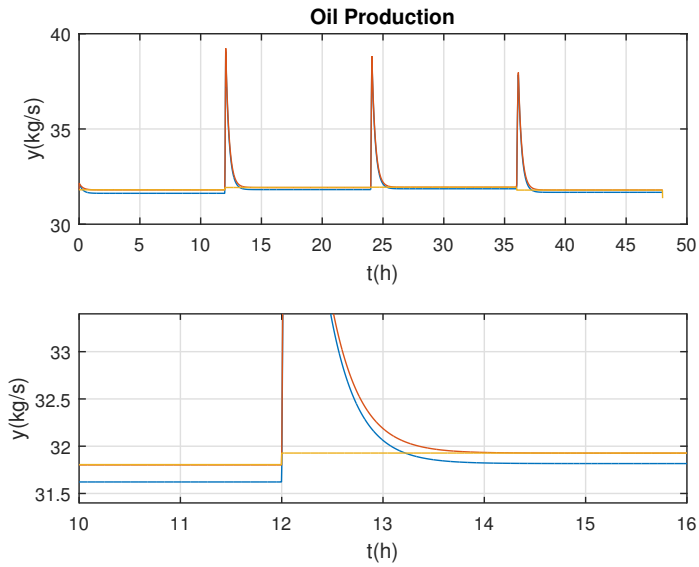

Figure 3.5: The oil production.

of adaptive control deal with known set points or references, however in several applications the goal is to find a set point that leads to a maximum output with an uncertain reference [54]. ESC was popular in the middle of twentieth century, but was nearly dormand for decades until its stability was proved in [54], regaining the interest for further developments and applications [72].

While it was usual to represent the plant as a static nonlinear map for ESC, in [54] the plant can be a general nonlinear dynamic system (possibly non-affine in control and open-loop unstable) whose reference-to-output equilibrium map has a maximum, and whose equilibria are locally exponentially stabilizable. Calli et al. [73] presented 5 categories of ESC: sliding mode, neutral network, approximation-

based, perturbation-based and adaptive. Among those the perturbation-based ESC is the most commonly used method through literature [73]. The extremum seeking method has seen remarkable advances during the past decade, including proof of local convergence, PID tuning, slope seeking, performance improvement and limitation in ESC and others [72].

In the following a general overview of the sinusoidal perturbation ESC is presented as well as a dither-free ESC scheme.

Sinusoidal Perturbation ESC Method

The operating principle of the sinusoidal perturbation ESC is illustrated by closed-loop system shown in Figure 3.6.

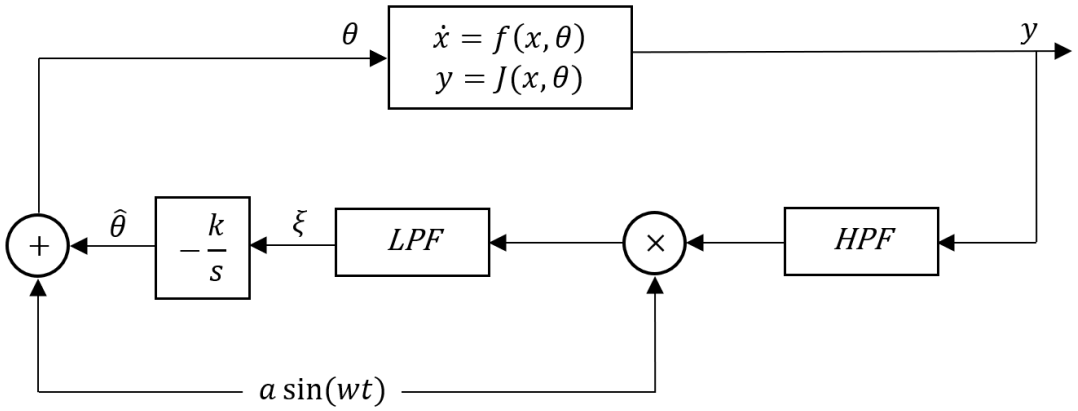

Figure 3.6: A peak seeking feedback scheme.

The system input is comprised by $\hat{\theta}$ plus a sinusoidal perturbation signal $a \sin wt$. $\hat{\theta}$ can be initially the best estimate of θ^*. If the perturbation is slow, plant is deemed static $y = h \circ l(\theta)$ and its dynamics do not interfere with the peek seeking scheme. The sinusoidal perturbation of the input essentially probes the slope of the objective function and it will generate a periodic response of y that can be either in phase or out of phase with the initial perturbation depending on the relationship with θ^*. It will be in phase if $\hat{\theta} < \theta^*$ and out of phase if $\hat{\theta} > \theta^*$. This is determined multiplying the output signal with DC components removed – a high-pass filter (HPF) is used for this purpose – by the sinusoidal perturbation. The multiplication of signals in phase will result in a mostly positive signal and if they are out of phase the result will be a mostly negative signal. In either case the product of the two sinusoids will have a DC component which will be extracted by the low-pass filter (LPF) . Then the integrator $(\frac{k}{s})$ is approximately the gradient update which tunes $\hat{\theta}$ to θ^*.

As shown in section 2.2.4 this method would require a very slow perturbation, i.e. a small frequency of the dither signal which makes this applicability not viable for gas-lifted oil application. The first order model derived from Eikrem's model

proposed by Peixoto et. al. [5] required a pre-compensation and a PLL in order to provide satisfactory results. Therefore, despite sinusoidal perturbation is a classic proven control scheme that works well under suitable conditions having been applied successfully in many practical applications, its not suitable for the current plant.

Dither-Free ESC Method

The sinusoidal perturbation represents one critical issue: the time-scale separation requirement in the ESC scheme. Knowing that a sinusoidal signal is required to allow a phase shift observation that leads ultimately to a gradient estimation, this estimate seems to be a very promising area of research that could be applicable to optimizing problems including ESC or not. In fact Krishnamoorthy et al. [64] presented a real-time optimization (RTO) introducing a new scheme based on controlling the estimated steady-state gradient of the costing function using feedback. This method claims to reach the optimum much faster than standard steady-state real-time optimization and significantly faster than classical ESC. Moreover it shoud be simpler in terms of tuning and to has reduced computational cost when compared to NMPC.

Other examples of this kind of approach can be found in literature. Noting that dither signal time-scale must be separated from the time-scale of the plant dynamics and the optimizer, it is likely that it limits the convergence speed of the algorithm. To overcome this issue, Hunnekens et al. [4] proposed a dither-free ESC scheme using 1st order least-square fits to estimate of the performance map. Instead of the dither signal, it utilizes a time window of history data of the performance curve to estimate its gradient. Figure 3.7 shows the scheme proposed at that time.

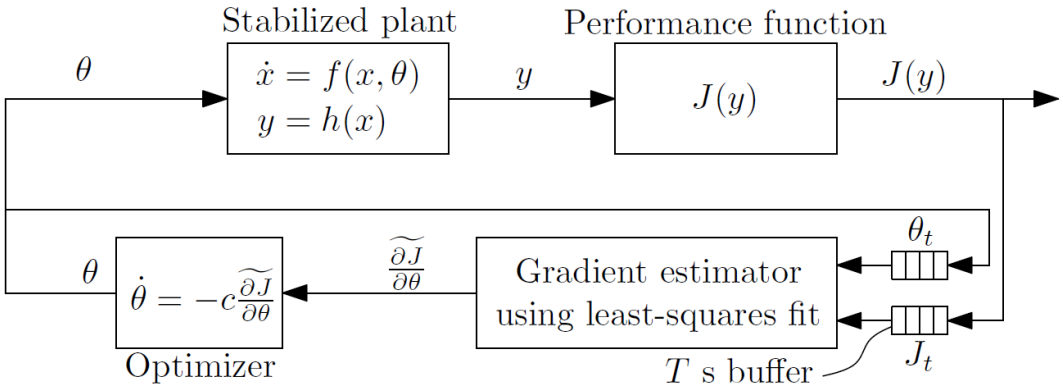

Figure 3.7: Dither-free ESC scheme with least-squares fit of last T seconds to estimate gradient [4].

This alternative approach will serve as basis for the controller proposed in next sections.

3.2.1 Problem Statement

Consider the second order approximation (2.49)–(2.51), repeated in the following for convenience:

$$\dot{x}_2 = u + r_{go}[c_1 x_2 + c_2 x_3 + c_3] - \frac{x_2}{x_3} y \,, \tag{3.41}$$

$$\dot{x}_3 = [c_1 x_2 + c_2 x_3 + c_3] - y \,, \tag{3.42}$$

$$y = w_{po}(x_2, x_3) \,, \tag{3.43}$$

where

$$[c_1 x_2 + c_2 x_3 + c_3] = w_{ro} = C_r \sqrt{\rho_o} \underbrace{\sqrt{p_r - p_{wh}}}_{\mu_{ro}} \,, \tag{3.44}$$

when the second scenario is considered. If the inner control loop is applied, then $x_2 \to x_2^d$, $x_3 \to x_3^d$, $\dot{x}_3 \to \dot{x}_3^d$ and $y \to w_{po}(x_2^d, x_3^d)$. Hence, from the close loop x_3-dynamics one can write approximately be described by:

$$\dot{x}_3^d \approx c_1 x_2^d + c_2 x_3^d + c_3 - w_{po}(x_2^d, x_3^d) \,,$$

as $t \to +\infty$. If $|\dot{x}_3^d|$ is sufficiently small, one can verify that $x_2^d = \psi(x_3^d)$, where $\psi(\cdot)$ is the $x_3 \times x_2$ static mapping. Therefore, one has

$$y(t) = w_{po}(\psi(x_3^d(t)), x_3^d(t)) = \Phi(x_3^d(t)) \,,$$

and $y(t)$ reaches the maximum for some $t \geq 0$ if: (i) $x_3^d(0) < x_3^*$ and $x_3^d(t)$ increases or; (ii) if $x_3^d(0) > x_3^*$ and $x_3^d(t)$ decreases.

Inspired by this property, the following ESC scheme is developed.

3.2.2 Proposed Dither-Free ESC and Numerical Simulations

The desired trajectory for the mass of oil in the tubbing be given by:

$$\dot{x}_3^d = k_m(1 + k_1 e^{-t/\tau_m}) u_{esc}(t) \,,$$

where $k_1 \geq 0$, $k_m > 0$ and $\tau_m > 0$ are design constants and $u_{esc}(t) \in \{1, -1\}$ is obtained in what follows.

Let $\mathcal{V}$, be a collection N equally time spaced samples of the output $y(t)$, i.e., $\mathcal{V} := \begin{bmatrix} y(t - N(h-1)) & \dots & y(t-h) & y(t) \end{bmatrix}^T$, where N is a design constant. Let $\mathcal{T} := \begin{bmatrix} t - N(h-1) & \dots & t-h & t \end{bmatrix}^T$ be the corresponding sampling time instants. By using least squares a polynomial $p(t)$, of order n_p, is obtained to interpolate $\mathcal{V}$,

as well as the corresponding time derivative $\dot{p}(t)$, where $n_p > 0$ is a design constant.

In order to robust estimate the gradient of the IO-mapping, the time derivative $\dot{p}(t)$ is evaluate in $\mathcal{T}$ (i.e., $\forall t \in \mathcal{T}$) and it is defined $\mathcal{N}(t)$ as the number of positive values of $\dot{p}(t)$ in the time window $\mathcal{T}$. Thus, if $\mathcal{N}(t) = N$ we say that the gradient is positive. Otherwise, if $\mathcal{N}(t) = 0$ we say that the gradient is negative. The following signal allows an estimate of the change of the gradient sign:

$$\xi(t) := 2\frac{\mathcal{N}(t)}{N} - 1 = \begin{cases} 1\,, & \mathcal{N}(t) = N\,, \\ -1\,, & \mathcal{N}(t) = 0\,, \\ g\,, & \mathcal{N}(t) \in (0, N)\,, \end{cases}$$

where $g \in (-1, 1)$. Thus, it is possible to detect the moment when $y(t)$ start to approximate the vicinity of the maximum value.

Let $T_\Delta > 0$ be a design time window where the control signal remains constant. The ESC control law is given by:

$$u_{esc}(t) = u_{esc}(t_k)\xi(t)\,, \quad \forall t \in (t_k, t_{k+1}]\,,$$

where $t_k = t_{k-1} + T_\Delta$, $t_0 = 0$, $k = 1, 2, \ldots$.

In the simulations, the following design constants were considered: $N = 1000$, $T_\Delta = 8.5$ hours, $\tau_m = 8640$, $k_m = 0.081$ and $k_1 = 4$. The inner control loop gains are: $K_2 = 0.1/20$ and $K_3 = 0.001$.

The ESC action is illustrated in Figure 3.8 with the time varying rate of change in the reference trajectory.The step response of the closed loop system can be observed in Figure 3.9, for the Eikrem's model and its second order approximation. In Figure 3.10, one can see the mass of gas in the tubbing increasing as x_3^d decreases. Note that overshoot appears due to the abrupt transition of the reference x_3^d and the high gain K_2. The corresponding time history of the gas injection control effort (w_{iv}) is given in Figure 3.11. The transient and steady state of the oil production is illustrated in Figure 3.12.

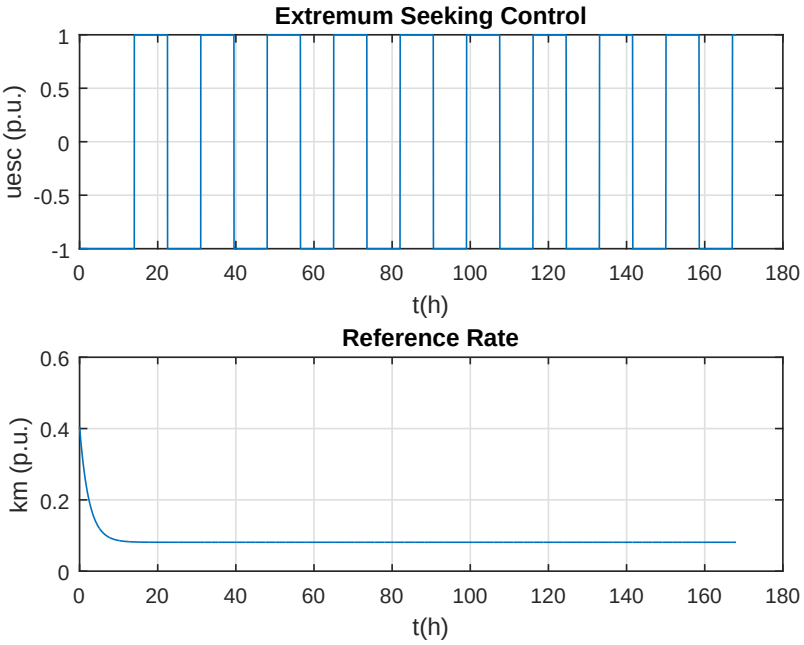

Figure 3.8: The ESC effort.

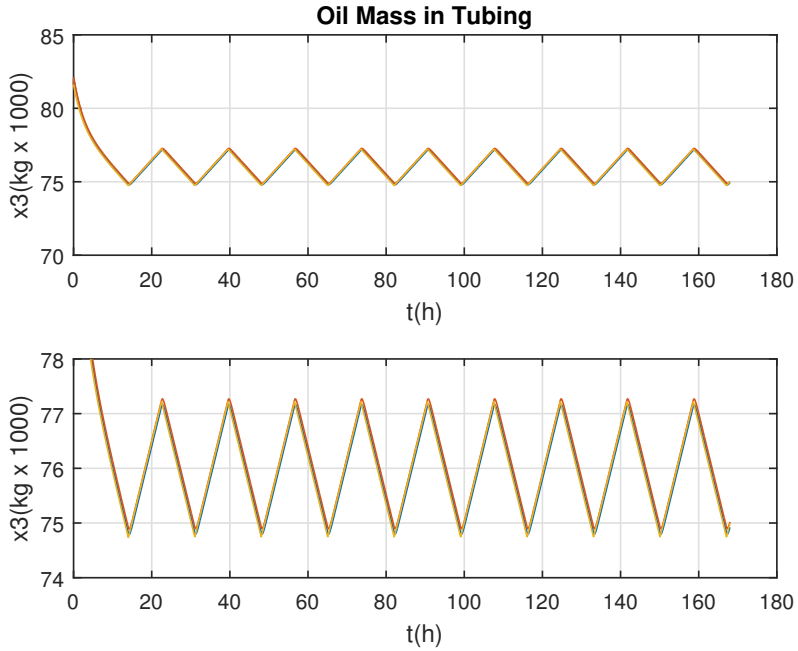

Figure 3.9: The mass of oil in the tubbing.

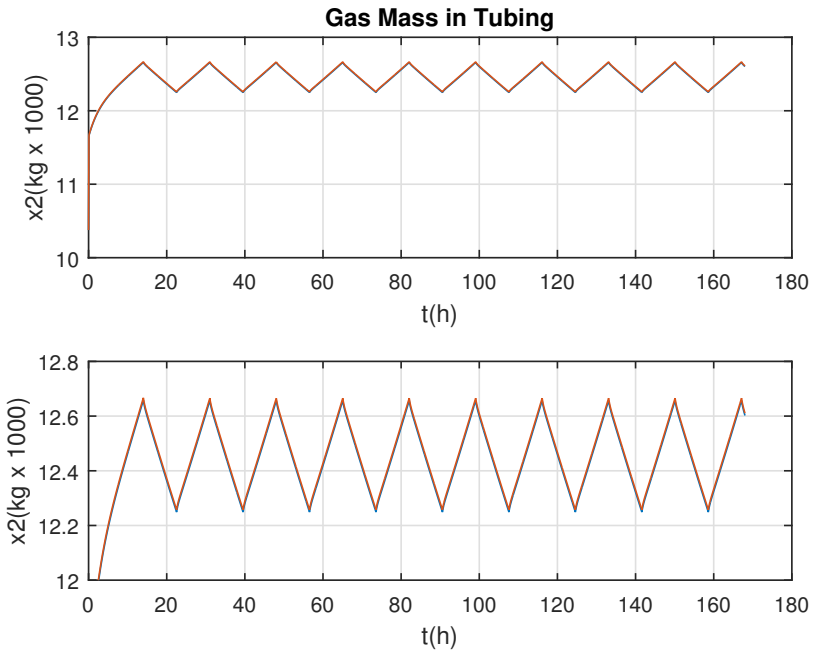

Figure 3.10: The mass of gas in the tubbing.

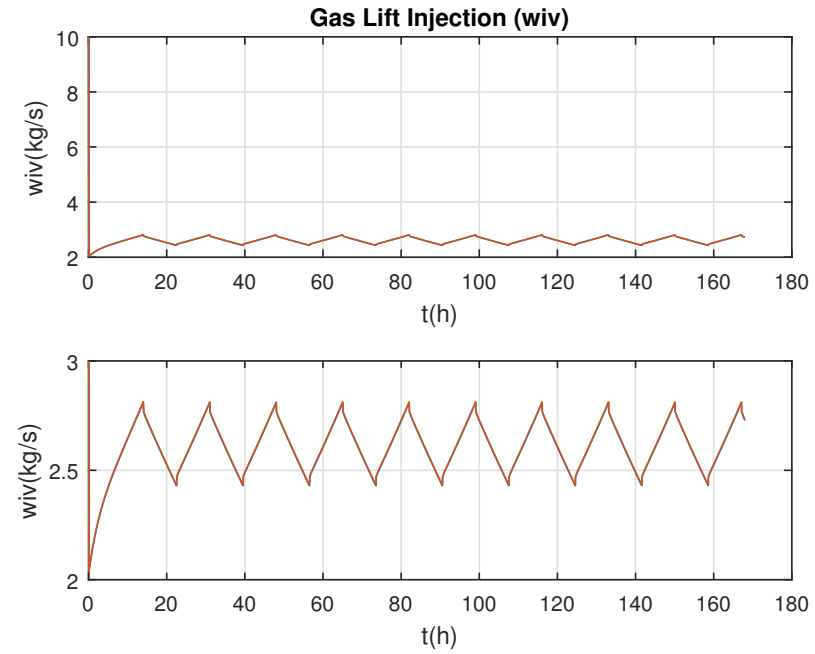

Figure 3.11: The control effort w_{iv}: gas injection.

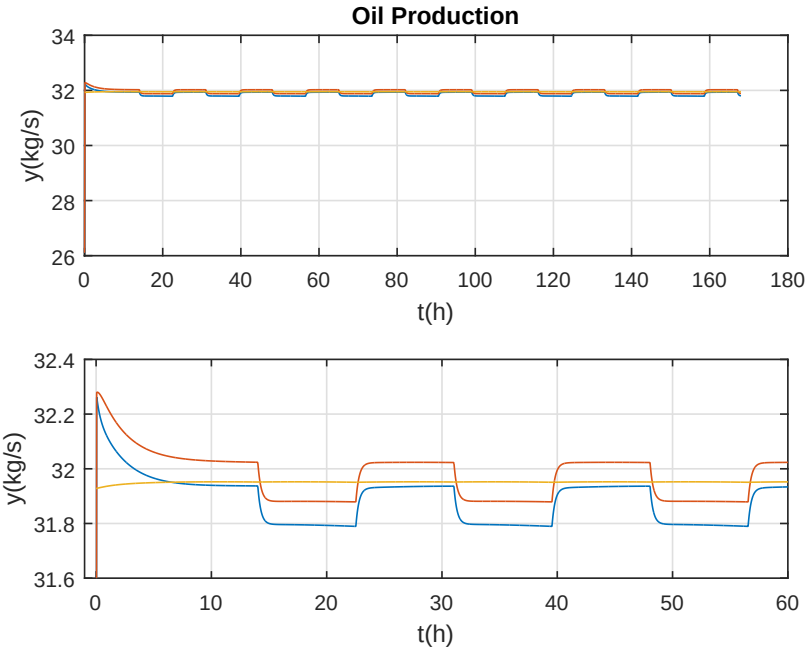

Figure 3.12: The oil production.

Chapter 4

Conclusion

This dissertation addressed a dither-free Extremum Seeking Control (ESC) design for oil production optimization in gas lifted wells to maintain the oil production around the optimum point of the Well Performance Curve (WPC). The gradient information was obtained via on-line curve fitting estimation. The main contributions of this dissertation was to propose a simplified second order model for gas-lifted oil wells based on the modified Eikrem's model and a new ESC scheme for oil production optimization, overcoming the low frequency limitation of the periodic perturbation ESC schemes required for this class of plants, due to the time scale separation. The use of a dither-free method allowed the removal of the perturbation time-scale from classic ESC schemes which makes it not viable for this application.

Additionally, a deep understanding of the process provided a suitable choice for the measured variables in order to estimate the system states. The optimization and control strategy was implemented in inner/outer control loop architecture, where an extremum seeking control governs the outer optimization loop and a nonlinear controller guarantees faster internal dynamics in the inner control loop. The greatest advantage of ESC for oil production environment is that it can overcome plant uncertainties to reach and keep production within a vicinity of the optimum point even if multiple parameters vary with time.Numerical simulations illustrated the performance of the proposed control schemes.

Future possible topics of research encompass an increase in complexity to get more accuracy on simulation results. There are also some simplifications to the model that could be further evaluated as the assumption of a two phase production flow. Some additional constraints like gas availability restrictions can be considered to address the fact of having an economical optimum different from the production peak of WPC. Moreover a controller applied for an entire production field could also be of much value. Lastly, a complete stability analysis could be performed, considering both inner and outer loops, the second order and the full order Eikrem's models.

Bibliography

[1] "Completion System for Gas Lift System". http://www.spadesintl.com/completion-systems-for-gas-lift-system, 2019. Accessed 20 Feb. 2019.

[2] EIKREM, G. O., AAMO, O. M., FOSS, B. A. "On Instability in Gas Lift Wells and Schemes for Stabilization by Automatic Control", *Society of Petroleum Engineers*, v. 23, May 2008.

[3] XAUD, A. F. S. *Modelagem, Simulação e Controle Via Busca Extremal de Poços Operando Por Gas-Lift.* Batchelor's Thesis, COPPE/UFRJ, Rio de Janeiro, Brazil, 2014.

[4] B.G.B.HUNNEKENS, HARING, M., H.NIJMEIJER. "A Dither-Free Extremum-Seeking Control Aproach using 1st-Order Least-Squares Fits For Gradient Estimation". Dec 2014.

[5] PEIXOTO, A. J., PEREIRA-DIAS, D., XAUD, A. F. S., SECCHI, A. R. "Modelling and Extremum Seeking Control of Gas Lifted Oil Wells", *IFAC Workshop on Automatic Control in Offshore Oil and Gas Production*, v. 2, May 2015.

[6] "Petroleum - Britannica Academic, Encyclopædia Britannica". https://academic-eb-britannica.ez29.capes.proxy.ufrj.br/levels/collegiate/article/petroleum/110438, 2018. Accessed 6 Feb. 2019.

[7] THOMAS, J. E. *Fundamentos de Engenharia de Petróleo.* 2 ed. Rio de Janeiro, Brazil, Interciência, 2004.

[8] BRUHN, C., GOMES, J., JR, C. L., JOHANN, P. "Campos Basin: Reservoir Characterization and Management - Historical Overview and Future Challenges", *Offshore technology Conference*, Jan 2003.

[9] HÜLSE, E. O. *Robust Production Optimization of Gas-Lifted Oil Fields.* Master's Thesis, UFSC, Florianópolis, Brazil, 2015.

[10] HU, B. *Characterizing Gas-Lift Instabilities*. dissertation, Norwegian University of Science and Technology, Trondheim, Norway, 2004.

[11] TEIXEIRA, A. F. *Otimização da Produção de Poços de Petróleo que Operam com Gas Lift Contínio*. Master's Thesis, Universidade Federal do Rio de Janeiro, Rio de Janeiro, RJ, Brazil, 2013.

[12] ELGSAETER, S. M., SLUPPHAUG, O., JOHANSEN, T. A. "A Structured Aproach to Optimizing Offshore Oil and Gas Production With Uncertain Models", *Computer and Chemical Engineering*, v. 34, n. 2, pp. 163–176, Feb 2010.

[13] BINDER, B. J. T. *Production Optimization in a Cluster of Gas-Lift Wells*. Master's Thesis, Norwegian University of Science and Technology, Trondheim, Norway, 2012.

[14] PINTO, A. C., BRANCO, C., DE MATOS, J., VIEIRA, P., DA SILVA GUEDES, S., JR., C. P., COELHO, A. D., CECILIANO, M. "Offshore Heavy Oil in Campos Basin: The Petrobras Experience", *Offshore Technology Conference*, May 2003.

[15] TOCAIMASA, G. J. V. *Production Optimization Oil Wells Advances in Extremun Seeking Control and Nonlinear Programming Tehcniques*. Master's Thesis, CEFET/RJ, Rio de Janeiro, Brazil, 2016.

[16] JANSEN, B., DALSMO, M., NØKLEBERG, L., HAVRE, K., KRISTIANSEN, V., LEMETAYER, P. "Automatic Control of Unstable Gas Lifted Wells", *SPE Annual Technical Conference and Exhibition*, Oct 1999.

[17] EIKREM, G., FOSS, B., IMSLAND, L., B. HU, M. G. "Stabilization of Gas Lifted Wells". In: *Proceedings of the 15th IFAC World Congress*, Barcelona, Spain, 2002.

[18] AAMO, O., EIKREM, G., SIAHAAN, H., FOSS, B. "Observer Design for Multiphase Flow in Vertical Pipes With Gas-Lift – Theory and Experiments", *Journal of Process Control*, v. 15, n. 3, pp. 247–257, Apr 2005.

[19] GANZAROLI, C. A. *Modelagem, simulação e controle da dinâmica de poços operando com gas-lift contínuo*. Master's Thesis, Universidade Federal de Santa Catarina, Florianópolis, 2011.

[20] SCIBILIA, F., HOVD, M., BITMEAD, R. R. "Stabilization of gas-lift oil wells using topside measurements". In: *Proceedings of the* 17^{th} *IFAC World Congress*, v. 41, pp. 13907–13912, Jul 2008.

[21] JAHANSHAHI, E., SKOGESTAD, S., HANSEN, H. "Control Structure Design for Stabilizing Unstable Gas-Lift Oil Wells", 8^{th} *IFAC Symposium on Advanced Control of Chemical Processes*, Jul 2012.

[22] RIBEIRO, C. H. P. *Controle Preditivo Multivariável em Plataformas Para a Produção de Petróleo Com Restrição de Qualidade.* Master's Thesis, Universidade Federal do Rio de Janeiro, Rio de Janeiro, RJ, Brazil, 2012.

[23] MUKHTYAR, V. A., SHASTRI, Y., GUDI, R. D. "Improved Stable, Optimal Production in Gas Lift Wells: Exploiting Additional Degrees of Freedom", 10^{th} *IFAC International Symposium on Dynamics and Control of Process Systems*, Dec 2012.

[24] PLUCENIO, A., M.CAMPOS, M., F.TEIXEIRA, A. "New Developments in the Control of Fluid Dynamics of Wells and Risers in Oil Production Systems". In: 2^{nd} *IFAC Workshop on Automatic Control in Offshore Oil and Gas Production*, v. 48, pp. 97–103, May 2015.

[25] MAHDIANI, M. R., KHAMEHCHI, E. "A novel model for predicting the temperature profile in gas lift wells", *Petroleum*, v. 2, pp. 408–414, Dec 2016.

[26] SHAO, W., BOIKO, I., AL-DURRA, A. "Plastic bag model of the artificial gas lift system for slug flow analysis", *Journal of Natural Gas Science and Engineering*, v. 33, pp. 573–586, Jul 2016.

[27] MORARI, M., LEE, J. H. "Model predictive control: past, present and future", *Computers & Chemical Engineering*, v. 23, pp. 667–682, May 1999.

[28] PLUCENIO, A., PAGANO, D. J., CAMPONOGARA, E., TRAPLE, A., TEIXEIRA, A. "Gas-lift Optimization and Control with Nonlinear MPC", *IFAC Proceedings Volumes (IFAC-PapersOnline)*, v. 7, Jan 2009.

[29] DIEHL, F. C., S.ALMEIDA, C., K.ANZAI, T., GEREVINI, G., S.NETO, S., MEIEN, O. F., C.M.M.CAMPOS, M., FARENZE, M., O.TRIERWEILER, J. "Oil production increase in unstable gas lift systems through nonlinear model predictive control", *Journal of Process Control*, v. 69, pp. 58–69, Sep 2018.

[30] PALKE, M. R., HORNE, R. N. "Optimization of Well Production Considering Gas Lift and Phase Behavior", *SPE Production Operations Symposium*, Mar 1997.

[31] NAKASHIMA, P. *Otimização de processos de produção de petróleo via injeção contínua de gás,*. PhD Thesis, UFSC, Santa Catarina, Brazil, 2004.

[32] SOUZA, J. N. M., DE MEDEIROS, J. L., COSTA, A. L. H., NUNES, G. C. "Modeling, simulation and optimization of continuous gas lift systems for deepwater offshore petroleum production", *Journal of Petroleum Science and Engineering*, v. 72, n. 3-4, pp. 277–289, Jun 2010.

[33] DOS SANTOS RIZZO FILHO, H. *A Otimização de Gás Lift na Produção de Petróleo: Avaliação da Curva de Performance do Poço*. Master's Thesis, COPPE/UFRJ, Rio de Janeiro, Brazil, 2011.

[34] CODAS, A., CAMPONOGARA, E. "Mixed-integer linear optimization for optimal lift-gas allocation with well-separator routing", *European Journal of Operational Research*, v. 217, n. 1, pp. 222–231, Feb 2012.

[35] RASHID, K., DEMIREL, S., COUËT, B. "Gas-Lift Optimization with Choke Control using a Mixed-Integer Nonlinear Formulation", *Industrial & Engineering Chemistry Research*, v. 50, pp. 2971–2980, Jan 2011.

[36] SAEPUDIN, D., SUKARNO, P., SOEWONO, E., SIDARTO, K. A., GUNAWAN, A. Y., SIREGAR, S., BUDICAKRAYANA, Y. "Optimization of Gas Injection Allocation in Multi Gas Lift Wells System", *International Conference on Engineering Optimization*, Jun 2008.

[37] CAMPONOGAR, E., PLUCENIO, A., TEIXEIRA, A. F., CAMPOS, S. R. "An automation system for gas-lifted oil wells: Model identification, control, and optimization", *Journal of Petroleum Science and Engineering*, v. 70, n. 3-4, pp. 157–167, Feb 2010.

[38] RASHID, K., BAILEY, W., COUËT, B. "A survey of methods for gas-lift optimization", *Modelling and Simulation in Engineering*, v. 2012, n. 24, Jan 2012.

[39] KRISHNAMOORTHY, D., FOSS, B., SKOGESTAD, S. "Real-Time Optimization under Uncertainty Applied to a Gas Lifted Well Network", *Processes*, v. 4, pp. 52, 12 2016.

[40] KRISHNAMOORTHY, D., FOSS, B., SKOGESTAD, S. "Gas Lift Optimization under Uncertainty", *Computer Aided Chemical Engineering*, v. 40, pp. 1753–1758, 01 2017.

[41] KRISHNAMOORTHY, D., AGUIAR, M. A., FOSS, B., SKOGESTAD, S. "A Distributed Optimization Strategy for Large Scale Oil and Gas Production Systems". In: *2018 IEEE Conference on Control Technology and Applications (CCTA)*, pp. 521–526, Aug 2018.

[42] KRISHNAMOORTHY, D., JAHANSHAHI, E., SKOGESTAD, S. "Gas-lift Optimization by Controlling Marginal Gas-Oil Ratio using Transient Measurements". In: 3^{rd} *IFAC Workshop on Automatic Control in Offshore Oil and Gas Production OOGP 2018*, v. 51, pp. 19–24, Jul 2018.

[43] S.GREMA, A., LANDA, A. C., CAO, Y. "Dynamic Self-Optimizing Control for Oil Reservoir Waterflooding". In: 2^{nd} *IFAC Workshop on Automatic Control in Offshore Oil and Gas Production*, v. 48, pp. 50–55, Florianópolis, Brazil, May 2015.

[44] ANS REZA KHANINEZHAD, S. N., JAFARPOUR, B. "A Generalized Formulation for Oilfield Development Optimization". In: 2^{nd} *IFAC Workshop on Automatic Control in Offshore Oil and Gas Production*, v. 48, pp. 56–61, Florianópolis, Brazil, May 2015.

[45] GRIMHOLT, C., SKOGESTAD, S. "Optimization of Oil Field Production Under Gas Coning Conditions Using the Optimal Closed-Loop Estimator". In: 2^{nd} *IFAC Workshop on Automatic Control in Offshore Oil and Gas Production*, v. 48, pp. 39–44, Florianópolis, Brazil, May 2015.

[46] DE PAULA, L. H., STORTI, F. C., FORTALEZA, E. "Sliding Control Applied to Subsea Oil and Gas Separation System under Fluid Transient Effects". In: 2^{nd} *IFAC Workshop on Automatic Control in Offshore Oil and Gas Production*, v. 48, pp. 33–38, Florianópolis, Brazil, May 2015.

[47] LARA, I. O. O. *Desenvolvimento de um Simulador Físico de Gás Lift Intermitente e Bombeio Pneumático Zadson em Escala de Laboratório.* Master's Thesis, UNICAMP, Campinas, Brazil, 2013.

[48] FALLER, A. C. *Desenvolvimento de uma Plataforma para Otimização da Produção em Tempo Real em Campos de Petróleo Operados por Gas-Lift.* Batchelor's Thesis, UFSC, Florianópolis, Brazil, 2009.

[49] GARCIA, A., ALMEIDA, I., SINGH, G., PURWAR, S., MONTEIRO, M., CARBONE, L., HEDEIRO, M. "An Implementation of On-line Well Virtual Metering of Oil Production", *SPE Intelligent Energy Conference and Exhibition*, Mar 2010.

[50] TAN, Y., MOASE, W. H., MANZIE, C., NESIĆ, D., MAREELS, I. "Extrmum Seeking From 1922 To 2010". In: *Proceedings of the 29th Chinese Control Conference*, Beijing, China, Jul 2010.

[51] HAMZA, M. H. "Extremum Control of Continuous Systems", *IEEE Transactions on Automatic Control*, v. 11, n. 2, pp. 182–189, Apr 1996.

[52] SPEYER, J. L., BANAVAR, R. N., CHICHKA, D. F., RHEE, I. "Extremum seeking loops with assumed functions". In: *Proceedings of the 39th IEEE Conference on Decision and Control*, v. 1, pp. 142–147, Dec 2000.

[53] OLALLA, C., ARTEAGA, M. I., LEYVA, R., AROUDI, A. E. "Analysis and Comparison of Extremum Seeking Control Techniques". In: *2007 IEEE International Symposium on Industrial Electronics*, pp. 72–76, Jun 2007.

[54] KRSTIĆ, M., WANG, H.-H. "Stability of Extremum Seeking Feedback for General Nonlinear Dynamic Systems", *Automatica*, v. 36, n. 4, pp. 595–601, 2000.

[55] KRSTIĆ, M. "Performance Improvement and Limitations in Extremum Seeking Control", *Systems & Control Letters*, v. 39, n. 5, pp. 313–326, 2000.

[56] ARIYUR, K. B., KRSTIĆ, M. *Real-Time Optimization by Extremum-Seeking Control*. 1 ed. United States of America, Wiley-Interscience, 2003.

[57] MANZIE, C., KRSTIĆ, M. "Extremum Seeking With Stochastic Perturbations", *IEEE Transactions on Automatic Control*, v. 54, n. 3, pp. 580–585, Mar 2009.

[58] HARING, M., JOHANSEN, T. A. "Asymptotic Stability of Perturbation-Based Extremum-Seeking Control for Nonlinear Plants", *IEEE Transactions on Automatic Control*, v. 62, n. 5, pp. 2302–2317, May 2017.

[59] VAN DE WOUW, N., HARING, M., NESIC, D. "Extremum-seeking control for periodic steady-state response optimization". pp. 1603–1608, Dec 2012.

[60] HAZELEGER, L., HARING, M., VAN DE WOUW, N. "Extremum-seeking control for steady-state performance optimization of nonlinear plants with time-varying steady-state outputs". In: *2018 Annual American Control Conference (ACC)*, pp. 2990–2995, Jun 2018.

[61] PEIXOTO, A. J., PEREIRA-DIAS, D., TOCAIMASA, G. J. V., OLIVEIRA, T. R. "Fast extremum seeking for a class of non Hammerstein-Wienner systems". In: *2017 American Control Conference (ACC)*, pp. 5666–5671, May 2017.

[62] KRISHNAMOORTHY, D., PAVLOV, A., LI, Q. "Robust Extremum Seeking Control with application to Gas Lifted Oil Wells", *IFAC-PapersOnLine*, v. 49, pp. 205–210, Dec 2016.

[63] PAVLOV, A., HARING, M., FJALESTAD, K. "Practical Extremum-Seeking Control for Gas-Lifted Oil Production", *2017 IEEE 56th Annual Conference on Decision and Control (CDC)*, v. 49, Dec 2017.

[64] KRISHNAMOORTHY, D., JAHANSHAHI, E., SKOGESTAD, S. "A Feedback Real Time Optimization Strategy Using a Novel Steady-State Gradient Estimate and Transient Measurements", *Industrial and Engineering Chemistry Research*, Dec 2018.

[65] KHALIL, H. K. *Nonlinear Systems*. 3 ed. New Jersey, Prentice Hall, 2002.

[66] PRITCHARD, P. *Introduction to Fluid Meachanics*. 8 ed. Hoboken, John Wiley & Sons, 2011.

[67] FRANTZEN, K. H., KENT, I., PHILIPS, R. "Control System Upgrades for Tordis and Vigdis Field - A Project Case Study of Revitalising Brownfield Developments with Next Generation Subsea Controls". In: *Offshore Technology Conference*, Jan 2011.

[68] "Subsea Instrumentation Interface Standardization". `https://siis-jip.com/`, 2019. Accessed 17 Feb. 2019.

[69] "Intelligent Well Interface Standardisation". `https://iwis-jip.com/`, 2019. Accessed 17 Feb. 2019.

[70] PIMENTEL, J., MACKENZIE, R., THIBAUT, E., GARNAUD, F. "Seamlessly Integrated Subsea All-Electric Systems: Laggan-Tormore as a Case Study". In: *Offshore Technology Conference*, May 2017.

[71] WINTHER-LARSSEN, E., MASSIE, D. "All-Electric as an Enabler for More Cost Effective Developments on Cluster Systems". In: *Offshore Technology Conference*, May 2017.

[72] LIU, S.-J., KRSTIC, M. *Stochastic Averaging and Stochastic Extremum Seeking*. 1 ed. London, Springer, 2012.

[73] CALLI, B., CAARLS, W., JONKER, P., WISSE, M. "Comparison of Extremum Seeking Control Algorithms for Robotic Applications". In: *IEEE International Conference on Intelligent Robots and Systems*, 10 2012.